Journal Pre-proof

IL-33 triggers early eosinophil-dependent events leading to metaplasia in a chronic model of gastritis-prone mice

Carlo De Salvo, Luca Pastorelli, Christine P. Petersen, Ludovica F. Buttò, Kristine-Ann Buela, Sara Omenetti, Silviu A. Locovei, Shuvra Ray, Hannah R. Friedman, Jacob Duijser, Wei Xin, Abdullah Osme, Fabio Cominelli, Ganapati H. Mahabeleshwar, Jason C. Mills, James R. Goldenring, Theresa T. Pizarro

PII: S0016-5085(20)35223-9
DOI: https://doi.org/10.1053/j.gastro.2020.09.040
Reference: YGAST 63791

To appear in: *Gastroenterology*
Accepted Date: 22 September 2020

Please cite this article as: De Salvo C, Pastorelli L, Petersen CP, Buttò LF, Buela K-A, Omenetti S, Locovei SA, Ray S, Friedman HR, Duijser J, Xin W, Osme A, Cominelli F, Mahabeleshwar GH, Mills JC, Goldenring JR, Pizarro TT, IL-33 triggers early eosinophil-dependent events leading to metaplasia in a chronic model of gastritis-prone mice, *Gastroenterology* (2020), doi: https://doi.org/10.1053/j.gastro.2020.09.040.

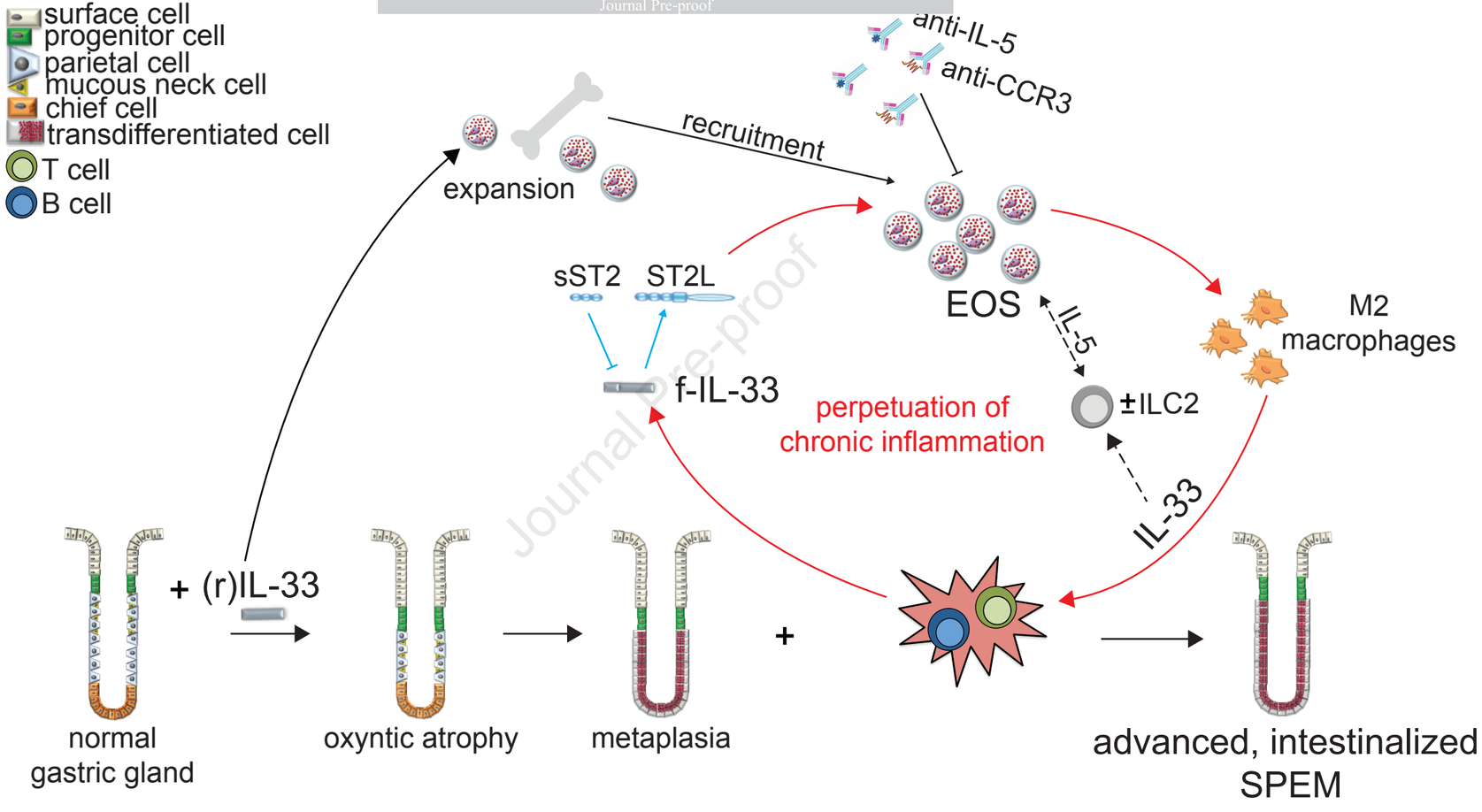

Title: IL-33 triggers early eosinophil-dependent events leading to metaplasia in a chronic model of gastritis-prone mice

Running title: IL-33 and eosinophils induce intestinalized SPEM

Carlo De Salvo[1], Luca Pastorelli[1,3], Christine P. Petersen[4], Ludovica F. Buttò[2], Kristine-Ann Buela[1], Sara Omenetti[1], Silviu A. Locovei[1,2], Shuvra Ray[1], Hannah R. Friedman[1], Jacob Duijser[1], Wei Xin[1], Abdullah Osme[1], Fabio Cominelli[2], Ganapati H. Mahabeleshwar[1], Jason C. Mills[5], James R. Goldenring[4], and Theresa T. Pizarro[1]

Departments of [1]Pathology and [2]Medicine/Division of Gastroenterology & Liver Disease, Case Western Reserve University School of Medicine, Cleveland, OH, 44106, USA; [2]IRCCS Policlinico San Donato, Gastroenterology & Gastrointestinal Endoscopy Unit, San Donato Milanese, 20097 and Department of Biomedical Sciences, University of Milan, Milan, 20122, Italy; [3]Department of Surgery and the Epithelial Biology Center, Vanderbilt University, Nashville, TN, 37235, USA; [4]Department of Medicine, Gastroenterology Division, Washington University School of Medicine, St. Louis, MO, 63110, USA

Grant support: This work was supported by grants from the NIH: DK056762, DK091222, DK042191, CA150964 Pilot & Feasibility Award (TTP), DK071590 (JRG), DK105129 (JCM), an NRSA F31 Predoctoral Fellowship (DK104600 to CPP), an Institutional T32 Fellowship from DK083251 (SL), as well as Cores from the Cleveland Silvio O. Conte Digestive Diseases Research Core Center (NIH DK097948). Other funding sources include the DeGregorio Family Foundation (TTP), the Department of Veterans Affairs: I01BX000930 (JRG), the Crohn's & Colitis Foundation: RFA326877, CDA581292 (CDS), RFA410354 (KAB), SRFA592800 (HRF), the American Gastroenterological Association: Eli & Edythe Broad Student Research Fellowship Award (HRF, JD), and the Italian Society of Gastroenterology (LP).

Abbreviations used in this paper: Apc, adenomatous polyposis coli; BM, bone marrow; CCR3, C-C motif chemokine receptor 3; CD44, cluster differentiation 44; CD163, cluster differentiation 163; Clu, clusterin; Fc, fragment crystallizable; GIF, gastric intrinsic factor; GSII, Griffonia simplicifolia lectin II; *H. pylori, Helicobacter pylori*; IgG, immunoglobulin; IHC, immunohistochemistry; ILC2, type 2 innate lymphoid cells; IL, interleukin; Il1rl1, interleukin-1 receptor-like 1; LP, lamina propria; MBP, major basic protein; PAS, periodic acid Schiff; PFA, paraformaldehyde; qPCR, quantitative polymerase chain reaction; SAMP, SAMP1/YitFc; SPEM, spasmolytic polypeptide-expressing metaplasia; TFF1/2, trefoil factor 1/2

Corresponding author: Theresa T. Pizarro, Ph.D., Department of Pathology, Case Western Reserve University School of Medicine, 2103 Cornell Road, WRB 5534, Cleveland, OH 44106, USA; Phone: 216-368-3306; Fax: 216-368-0494; Email: theresa.pizarro@case.edu

Conflict of interest: The authors have no conflict(s) of interest to disclose

Author contribution: *CDS*-data acquisition, analysis/interpretation, drafting/critical revision of manuscript for important intellectual content, obtained funding; *LP*-data acquisition, analysis/interpretation, drafting/critical revision of manuscript for important intellectual content; *CPP*-data acquisition, analysis/interpretation; *LFB*-data acquisition, analysis/interpretation; *KAB*-data acquisition, analysis/interpretation, obtained funding; *SO*-data acquisition; *SL*-data acquisition/analysis; *SR*-data acquisition; *HRF*-data acquisition, obtained funding; *JD*-data acquisition, obtained funding; *WX, AO*-data analysis/interpretation of data; *FC*-data acquisition, material support; *GHM*-data acquisition, analysis/interpretation, material support; *JCM*-material support, critical revision of manuscript for important intellectual content; *JRG*-material support, data analysis/interpretation, critical revision of manuscript for important intellectual content, study supervision; *TTP*-study concept and design, data analysis/interpretation, critical revision of manuscript for important intellectual content, obtained funding, overall study supervision.

Acknowledgements

Personnel: We thank the following individuals for their important contributions to the manuscript – Xiao-Ming Wang, Danian Che, Hannah L. Havran, and Brian Marks for their technical support, as well as James J. Lee and Dirk E. Smith for provision of important reagents.

Abstract

Background & Aims. IL-33/IL-1F11 is an important mediator for the development of Th2-driven inflammatory disorders and has also been implicated in the pathogenesis of GI-related cancers, including gastric carcinoma. We therefore sought to mechanistically determine IL-33's potential role as a critical factor linking chronic inflammation and gastric carcinogenesis using gastritis-prone SAMP1/YitFc (SAMP) mice. *Methods*. SAMP and (parental control) AKR mice were assessed for baseline gastritis and progression to metaplasia. Expression/localization of IL-33 and its receptor, ST2/IL-1R4, were characterized in corpus tissues, and both activation and neutralization studies were performed targeting the IL-33/ST2 axis. Dissection of immune pathways leading to metaplasia were evaluated, including eosinophil depletion studies using anti-IL-5/anti-CCR3 treatment. *Results*. Progressive gastritis and ultimately, intestinalized spasmolytic polypeptide-expressing metaplasia (SPEM) was detected in SAMP stomachs, which was absent in AKR, but could be moderately-induced with exogenous, recombinant (r)IL-33. Robust peripheral (bone-marrow, BM) expansion of eosinophils and local recruitment of both eosinophils and IL-33-expressing M2 macrophages into corpus tissues were evident in SAMP. Interestingly, IL-33 blockade did not affect BM-derived expansion and local infiltration of eosinophils, but markedly decreased M2 macrophages and SPEM features, while eosinophil depletion caused a significant reduction in both local IL-33-producing M2 macrophages and SPEM in SAMP. *Conclusions*. IL-33 promotes metaplasia and the sequelae of eosinophil-dependent downstream infiltration of IL-33-producing M2 macrophages leading to intestinalized SPEM in SAMP, suggesting that IL-33 represents a critical link between chronic gastritis

and intestinalizing metaplasia that may serve as a potential therapeutic target for pre-neoplastic conditions of the GI tract.

Keywords: IL-33/ST2 axis, M2 macrophages, SPEM/intestinalized SPEM, gastric cancer

Introduction

The link between chronic inflammation and cancer is well established, with inflammation-associated cancers among the most highly represented and frequently-occurring neoplasias worldwide[1,2]. Investigation over the last several years has focused on determining critical pathways involved in this process, with a number of candidate molecules identified, including members of the interleukin-1 (IL-1) family that are particularly important in GI-related cancers[3,4]. Of these, IL-33 plays a prominent role in intestinal tumorigenesis, both in mouse models of adenomatous polyposis (*i.e.*, *Apc*^{Min} strain) and inflammation-associated colorectal cancer, as well as in patients with colorectal adenocarcinoma[5,6,7]. Less is known regarding IL-33's contribution to the development of upper GI cancers, including gastric adenomas, which generally occur as a consequence of chronic gastritis after prolonged *Helicobacter (H.) pylori* infection or as a result of autoimmune gastritis[8]. As such, while IL-33 clearly plays a paramount role in both inflammation and cancer, a definitive link between IL-33-dependent inflammation and carcinogenesis in the GI tract has yet to be determined.

IL-33/IL-1F11 is widely distributed throughout various organ systems, primarily in non-hematopoietic cells, but also in cells of hematopoietic origin, particularly in restricted populations of professional antigen presenting cells, such as macrophages[9,10]. IL-33 was initially associated with Th2 immunity, based on expression of its cell-bound receptor, ST2L/IL-1R4, on polarized Th2 lymphocytes[9] and more recently, on group 2 innate lymphoid cells (ILC2s)[11], and its ability to effectively induce M1, but more commonly M2, macrophage differentiation[12]. Importantly, IL-33 also potently activates

and induces eosinophil infiltration into mucosal organs that interface with the external environment, such as the GI and respiratory tracts[9,13,14].

Relevant to the present study, prior reports associate IL-33 with poor prognosis in gastric cancer patients[15], and *in vitro* experiments suggest that IL-33 confers chemoresistance[16], and increased invasiveness[17] of gastric cancer cells. Recently, IL-33-dependent activation of mast cells was shown to promote tumor angiogenesis and growth that, in combination with tumor-associated macrophages, positively correlates with decreased survival of gastric cancer patients[18]. As such, although evolving, the precise role of IL-33 in gastric cancer has not yet been fully elucidated; specifically, how IL-33 mechanistically exerts the aforementioned effects, and whether IL-33 contributes to the development of pre-neoplastic states ultimately leading to gastric cancer.

In fact, chronic inflammatory conditions of the stomach often result in reactive modifications of the mucosa, including atrophy of mature acid-secreting cells as new metaplastic lineages arise. Such metaplastic changes in epithelial cells increase the risk of developing dysplasia and gastric cancer[19-21]. The initial metaplasia that arises, concomitant with acid-secreting parietal cell atrophy, is defined by the existence of antral-like mucous cells within the body (corpus) of the stomach and is known as spasmolytic polypeptide expressing metaplasia (SPEM), or pseudopyloric metaplasia. SPEM[22] is thought to arise from reprogramming of mature chief cells after parietal cell loss[23-25] and is thus named by the induced expression of spasmolytic polypeptide, *i.e.*, trefoil factor 2 (TFF2), in metaplastic cells[23,26-28]. In addition to SPEM, the stomach can undergo intestinal metaplasia[19], which is confirmed by the presence of intestinal lineages, such as mucus-secreting goblet cells. Chronic inflammation can promote the

progression of metaplastic mucosa to a more proliferative phenotype that is at risk for progression to dysplasia and cancer[29]. Experimentally, SPEM can be chemically-induced by L635, a parietal cell-specific protonophore, that generates a cascade of events leading to oxyntic atrophy, infiltration of activated M2-polarized macrophages, and SPEM that can develop intestinal characteristics in mice[30]. Using this model, IL-33 promotes IL-13-dependent M2 polarization of recruited macrophages and the development of SPEM[31].

In the present study, we evaluate a murine model that spontaneously develops *chronic* gastric inflammation, *i.e*., SAMP1/YitFc (SAMP) strain[32], to uncover potential IL-33-dependent mechanism(s) leading to, and downstream of, parietal cell loss and chief cell transdifferentiation, that can result in SPEM, and an even more proliferative, intestinalized SPEM. We show that: a) gastritis-prone SAMP progressively develop metaplasia leading to advanced SPEM-like features, b) exogenous rIL-33 administration induces moderate metaplasia and M2 macrophage infiltration in stomachs of healthy, (AKR) mice, and under chronic inflammatory conditions, exacerbates and advances metaplasia-acquiring intestinal characteristics in SAMP, c) neutralization of IL-33 in SAMP with established disease dampens gastritis and progression of metaplasia/SPEM, and d) IL-33 induces potent peripheral eosinophil expansion and subsequent recruitment into stomachs of treated mice, while e) eosinophil depletion markedly diminishes M2 macrophage infiltration and SPEM-like features in SAMP. Together, our data suggest that IL-33 plays a central role in the early events leading to SPEM and that during chronic inflammation, and/or perhaps under other predisposing conditions that promote lack of immune tolerance, IL-33-dependent eosinophil activation

and migration are essential for this process to occur. As such, targeting the IL-33/ST2 axis for therapeutic purposes may be beneficial for the treatment and/or prevention of pre-neoplastic states leading to gastric cancer.

Materials and Methods

Mice. Mice were provided through core services supported by the Animal and Mouse Models Cores of NIH P01 DK091222 and P30 DK097948, respectively. SAMPx*Il33*$^{-/-}$ mice were developed by backcrossing male C57BL/6J (B6) mice homozygous for a null allele of *Il33* (*Il33*$^{-/-}$)[5,33] with female SAMP for 10 generations, and validated by microsatellite analysis comparing SAMP- vs. B6-specific markers. Breeding of F_1N_{10} heterozygous offspring generated SAMP homozygous *Il33*$^{-/-}$, heterozygous, and WT controls, identified by PCR[5,33]. Mice were maintained as previously described[34], with all procedures approved by CWRU's IACUC.

Tissue harvest and histologic/SPEM assessment. Mice were euthanized and whole stomachs removed and opened along the greater curvature. Forestomach and antrum were excised, and corpus dissected along the longitudinal plane with one strip each placed in RNA*later*® (Ambion®, ThermoFisher Scientific, Waltham, MA) or RIPA buffer (Pierce Biotechnology, Rockford, IL), and maintained at -20°C until later RNA and protein extraction, respectively. Remaining tissue strip was submerged in either Bouin's (Ricca Chemical Company, Arlington, TX), 4% PFA (ChemCruz, Biotechnology, Inc., Dallas, TX) or methacarn. Bouin's/PFA- and methacarn-fixed tissues were rinsed in 70% ethanol after 24h or 20 min, respectively, processed, paraffin-embedded, and sectioned at 3-4µm. Specimens were stained with either H&E or Alcian Blue/PAS with optional hematoxylin 7221 (Thermo Scientific™ Richard-Allan Scientific™, Kalamazoo,

MI). Samples were evaluated by trained GI pathologists (WX, AO) in a blinded-fashion for gastritis/epithelial alterations and SPEM/intestinalized SPEM as previously described[30,32]. SPEM was scored by calculating percentage cross-sectional involvement, defined by oxyntic atrophy with loss of parietal cells and replacement of gastric glands with mucous cell lineages staining positive for PAS/Alcian blue.

***In vivo* studies.** Experiments were conducted in a blinded manner, with mice randomized to different interventions using progressive numeric labeling, the code only known to animal caretakers and revealed at end of each experiment. Scientific rigor, data reproducibility and biological variables were followed, based on recently published guidelines[35]. SAMP and gender/age-matched AKR were evaluated for baseline gastritis and progression to SPEM/intestinalized SPEM[30,32]. For exogenous IL-33 experiments, 8- to-12-wk-old mice were i.p.-injected with either rIL-33 (33μg/kg) (Enzo Life Sciences, Farmingdale, NY) or HBSS (vehicle), daily for 1-wk. IL-33 neutralization was achieved using a fusion protein (5 mg/kg, i.p. 2X/wk for 4-wks) consisting of the extracellular domain of mouse soluble (s)ST2 fused to IgG1-Fc (sSt2-Fc); controls were similarly administered IgG1-Fc (Dirk E. Smith, Amgen, Inc., Seattle, WA). Eosinophil depletion was performed using monoclonal antibodies against IL-5 and CCR3, and controls treated with an isotype IgG[34].

qRT-PCR and Western blots. Total RNA was isolated, reverse-transcribed, and qPCR performed as previously described[34], using specific target gene primers (**Supplemental Table 1**), normalized to β-actin or *36B4*, and reported as relative fold-difference among groups, with baseline/controls set arbitrarily at 1. Total protein extracts from corpus were prepared and Western blotting performed[10,33].

BrdU staining and Immunohistochemistry (IHC). Mice were injected with BrdU labeling agent (Invitrogen, Carlsbad, CA) 2h before euthanization, gastric tissues harvested, fixed in 4% PFA, and stained following manufacturer's instructions (BrdU Staining Kit; Invitrogen). IHC was performed using either a polyclonal goat anti-mouse IL-33 IgG (R&D Systems, Minneapolis, MN), biotinylated *Dolichos biflorus* agglutinin (DBA, Vector Laboratories, Burlingame, CA), or a monoclonal rat anti-mouse MBP IgG (clone MT-14.7) (James J. Lee, Mayo Clinic, Scottsdale, AZ), with negative controls prepared under identical conditions in the absence of respective primary antibodies[34]. Parietal cell/eosinophil counts were calculated by average intact, nucleated cells positive for DBA/MBP in 10 randomly-selected HPFs[34]. Immunofluorescence for confocal imaging was performed to detect GSII, CD44v, Clu, CD163, IL-33, GIF, and imaged/analyzed by the Vanderbilt Digital Histology Shared Resource[31].

Flow Cytometry. BM from femurs/tibias were harvested and processed as previously described[34]. Corpus tissues were processed into single-cell suspensions[31]. 2 x 10^6 cells were stained with LIVE/DEAD Fixable Near-IR Dead Cell Stain (ThermoFisher Scientific), and specific antibodies to detect eosinophils and M2 macrophages (**Supplemental Table 2**). Samples were acquired with a BD LSR II flow cytometer and data analyzed with FlowJo Software (both, Becton Dickinson)[31,34].

Statistical analyses. Data were analyzed using GraphPad Prism 5 (GraphPad Software, Inc., La Jolla, CA). Selection of appropriate statistical tests was based on variance and underlying distribution of data. Global effects between groups were assessed using one-way ANOVA with Bonferroni correction for multiple comparisons. Differences between individual groups were directly compared using two-sample

unpaired Student's t-test and results expressed as mean±SEM, unless otherwise indicated, with $P<0.05$ considered significant.

Results

Gastritis-prone SAMP exhibit morphologic features and a molecular profile consistent with intestinalized SPEM

SAMP mice develop chronic, immune-mediated gastritis with increased severity over time[32]. Stomachs from 20-wk-old SAMP show remarkable and progressive parietal cell loss compared to age-matched AKR controls, which possess abundant parietal cells (**Fig. S1A**). The emergence of prominent Alcian blue/PAS-stained hyperplastic mucous neck cells in SAMP highlight the presence of acidic mucins, commonly found in SPEM and adenocarcinoma[36], but are absent in AKR (**Fig. S1A**). Older SAMP display intense staining for the mucous marker, Griffonia simplicifolia II (GSII) lectin, while co-localization with either Cd44v or clusterin (Clu), indicative of SPEM, shows more intense Clu expression along the gastric glands compared to AKRs; the presence, albeit subtle, of Cd44v at the base of gastric glands in 20-wk-old SAMP is also detected, but virtually absent in the other experimental groups (**Fig. S1B**).

Molecular profiling of full-thickness corpus shows a striking decrease in expression of genes associated with oxyntic atrophy and foveolar hyperplasia, including gastric intrinsic factor (*Gif*), ATPase H+/K+ transporting alpha subunit (*Atp4a*), and trefoil factor 1 (*Tff1*), comparing SAMP vs. AKR, particularly in older mice (**Fig. S2A**). During acute oxyntic atrophy, as parietal cells die, chief cells show a rapid decrease in the zymogen granule maturation transcription factor, *Mist1*, and an increase in *Tff2*[26,37]. While no differences in *Tff2* are detected among experimental groups, *Mist1* is markedly

decreased in SAMP vs. AKR **(Fig. S2B)**. Furthermore, the SPEM markers, human epididymus protein 4 (*He4*), *Clu*, lysozyme (*Lyz*), and glutathione peroxidase 2 (*Gpx2*)[29,37], are all dramatically increased in SAMP with established disease vs. AKR **(Fig. S2C)**. Importantly, markers of more advanced, proliferative lesions (intestinalized SPEM)[29,30], including cystic fibrosis transmembrane conductance regulator (*Cftr*) and deleted in malignant brain tumors protein 1 (*Dmbt1*), are strongly upregulated in 20-wk-old SAMP vs. AKR, while the early tumor shrinkage variant 5 (*Etv5*) transcription factor is unchanged (**Fig. S2D**).

Increased circulating IL-33, with its most bioactive form localizing to gastric M2 macrophages in SAMP with advanced SPEM

To test the hypothesis that increased and persistent exposure to IL-33 may be needed for intestinalized SPEM to occur, we initially measured systemic/circulating IL-33, which is substantially increased in SAMP, even prior to histologically-evident gastritis (at 4-wks) and dramatically rises as disease becomes more severe, compared to IL-33 in AKR that remains relatively stable (**Fig. S3**). Locally, within non-diseased stomachs of 4-wk-olds, IL-33 is primarily found in foveolar epithelium, almost exclusively localized to nuclei (**Fig. 1A**). In older mice, AKR retain some epithelial-specific nuclear expression with scant IL-33^{+} cells within the lamina propria (LP), while abundant and diffuse IL-33 immunoreactivity is observed in SAMP, also within the LP, as well as at the base of the mucosa (**Fig. 1A**). Evaluation of IL-33 isoforms reveals less abundant IL-33 in 4-wk-old SAMP compared to AKR; however, in older SAMP, only full-length IL-33 (fIL-33), representing its most bioactive 30kD form[38], is prominently expressed, while other, less bioactive forms[39,40] are present in AKR (**Fig. 1B**). In fact, SAMP express

mainly fIL-33, whereas the 20-22 kD cleaved form (cIL-33) is virtually undetectable, but clearly present in AKR (**Fig. 1B**), suggesting increased release of bioactive fIL-33 in SAMP with established disease. Surprisingly, *Il33* in SAMP stomachs is decreased compared to AKR (**Fig. 1C**), which may be due to high circulating IL-33 levels (**Fig. S3**) and potential negative feedback mechanism(s) downregulating IL-33's bioactivity. Finally, to identify the cellular source of the considerable, yet diffuse, IL-33 staining within the gastric submucosa of older SAMP (**Fig. 1A**), immunofluorescent co-localization studies were performed, revealing abundant, infiltrating IL-33-expressing $CD163^+$ M2 macrophages that are virtually absent in non-inflamed AKR, but can be elicited with rIL-33 (**Fig. 1D**). Phenotypic characterization of SAMP gastric mucosal cells confirm the presence of IL-33-producing M2 macrophages (**Figs. S4** and **1E-F**), with an overall dominant M2 vs. M1 profile vs. AKR **(Fig. S5**).

Exogenous administration of IL-33 induces SPEM in normal (AKR) mice

One of the original observations regarding IL-33's bioactivity was its ability to promote epithelial hyperplasia, mainly in goblet cells, within GI and airway mucosae[9]. These findings were confirmed in stomachs of IL-33-treated B6 mice, which results in a Th2/STAT3-driven gastric pathology[41]. Aside from inducing infiltration of IL-33-expressing $CD163^+$ M2 macrophages (**Fig. 1D**), acute systemic exposure of IL-33 AKR consistently promotes the gross anatomical appearance of thickened gastric mucosal folds that are absent in vehicle-treated mice (**Fig. 2A**). Histologic evaluation of these folds reveal striking alterations, including overall hypertrophy of the gastric mucosa, epithelial hyperplasia, as well as oxyntic atrophy, while parietal and chief cells remain relatively intact in vehicle-treated AKR (**Fig. 2A**). Interestingly, although exogenous IL-

33 results in only 25% of AKR displaying significant gastritis, increased epithelial hyperplasia suggests its contribution to inducing mucous neck cell hyperplasia and metaplasia (**Fig. 2B**). The presence of metaplasia is further characterized by prominent proliferation of cells within the gastric glands, demonstrated by a greater number of $BrdU^+$ cells, along the neck and at the base of gastric glands (**Fig. 2A**, right panels), and Alcian blue/PAS staining, highlighting the appearance of hyperplastic acidic mucin-producing neck cells, comparing IL-33- vs. vehicle-treated AKRs (**Fig. 2C**). Finally, accumulation of GSII lectin (a surrogate for MUC6 expression) co-localizing with Cd44v at the base of glands in treated AKR (**Fig. 2C**), indicating chief cells transdifferentiation[42], also supports the development of IL-33-dependent SPEM (**Fig. 2D**), but for the most part, in the absence of inflammation.

Consistent with oxyntic atrophy, molecular profiling shows that *Gif* and *Atp4a* are downregulated in corpus tissues from IL-33-treated AKR (**Fig 3A**), and while *Tff1* shows a trend towards decreased expression, *Tff2* is strongly upregulated following short-term IL33 exposure (**Fig. 3A**), further indicating the occurrence of IL-33-induced chief cell transdifferentiation leading to SPEM. Additionally, *He4* and *Clu* are consistently upregulated after rIL-33 (**Fig. 3B**); however, only *Cftr* is considerably increased for the intestinalized SPEM markers assayed (**Fig. 3C**), suggesting that IL-33 has a prominent effect on the development of SPEM but, in order to progress to a more advanced intestinalized phenotype, a longer, more chronic exposure to IL-33 may be needed. Interestingly, exogenous IL-33 does not affect *Il1rl1* (ST2L), encoding the signaling receptor for IL-33, but *Il1rl1* (sST2), encoding soluble ST2, an IL-33-specific decoy receptor[43], is markedly increased and *Il33* is significantly decreased (**Fig. 3D**), which is

similar to what is observed in SAMP with established disease, and may represent a negative feedback response after rIL-33.

Blockade of IL-33 signaling dampens SPEM progression in SAMP mice

To test whether IL-33 neutralization is effective in dampening and/or reversing intestinalized SPEM, we administered sST2-Fc to SAMP with established disease. Treatment with sST2-Fc reduces expression of Cd44v, and does not appear to change GIF compared to vehicle controls, but has a significant impact on diminishing the number of IL-33-producing $CD163^{+}$ M2 macrophages, as well as GSII expression (**Fig. 4A**, right panels). Histologically, global improvement is evident in regards to epithelial architecture and gland structure, with decreased Alcian blue/PAS-stained cells, indicating diminished production of acidic mucins. A substantially increased census of cells positive for the parietal cell-specific marker, DBA, is also observed, consistent with morphology of parietal cell precursors (**Fig. 4A-B**), which dramatically arise during restitution from SPEM[44]. Histologic evaluation shows a 57% decrease in epithelial hyperplasia following IL-33 blockade (**Fig. 4C**), suggesting restorative epithelial processes towards normal homeostasis.

Histology images also show that overall gastric inflammation is visibly decreased after IL-33 blockade vs. control, confirmed by reduction in total inflammatory scores (**Fig. 4D**). Of note, the primary component driving total inflammation downward in sST2-Fc-treated SAMP is chronic inflammation, which decreases by 41%, and not acute inflammation, which remains relatively unchanged between experimental groups (**Fig. 4D**).

Peripheral expansion and local recruitment of eosinophils are dramatically increased in SAMP with advanced SPEM and rely on IL-33

We previously reported that eosinophils play a central role in mediating chronic, Th2-driven ileitis that is dependent on intestinal IL-33 induced by the gut microbiome[34]. In the present study, we found that expansion of peripheral BM-derived eosinophils, defined as CD11b^{+}Siglec-F^{+} cells (**Fig. S6**), is already present in 4-wk-old SAMP, prior to the appearance of gastritis, compared to age-matched AKR (**Fig. 5A**). This trend is consistent with what was previously observed in older SAMP[34], when intestinal-like metaplasia is fully established, and is increased vs. 4-wk-olds. Locally, baseline presence of eosinophils identified by MBP, one of the most prevalent proteins specifically-produced by eosinophils[45,46], is detected in young SAMP, and also found in equal numbers in age-matched AKR (**Fig. 5B**). As disease progresses, the number of infiltrating MBP^{+} eosinophils greatly increases, first appearing at the margination between submucosa and muscularis mucosa, and then collecting at the base of the gastric glands with infiltrates percolating upwards throughout the LP vs. AKRs, wherein eosinophils are scarce and sparsely detected (**Fig. 5B**). Quantitatively, MBP^{+} eosinophils are clearly evident in SAMP corpus as intestinalizing SPEM progresses, showing a 4-fold increase by 20-weeks compared to AKR (**Fig. 5B**). These results indicate that systemic expansion of eosinophils and their recruitment into gastric tissues occurs early and are sustained in SAMP with advanced, intestinalized SPEM. Significant abrogation of BM-derived eosinophils (**Fig. 5A**) and subsequent decreased recruitment into the gastric mucosa of SAMP lacking IL-33 (SAMPx*Il33*$^{-/-}$) compared to

WT littermates (SAMPx*Il33*$^{+/+}$) (**Fig. 5C**) confirm the early reliance on IL-33 for these effects.

Eosinophil expansion, in fact, can be dramatically elicited, particularly in the periphery, in healthy AKR after acute (one-wk) IL-33 administration. Likewise, aside from the striking mucosal epithelial alterations described above (**Fig. 2**), IL-33 also promotes a trend of eosinophil recruitment into the corpus of treated AKR (**Fig. 5D**). These results indicate that, in the absence of inflammation, exogenous IL-33 induces robust systemic expansion, and to a lesser extent, local recruitment, of eosinophils into the gastric mucosa. Interestingly, IL-33 blockade in SAMP with established disease does not affect expansion of BM-derived eosinophils (**Fig. 5A**) or local recruitment of MBP^{+} eosinophils (**Fig. 5E**), indicating that once these processes are induced, particularly in mice exposed to chronic inflammatory conditions, they cannot be reversed.

Eosinophil depletion effectively reduces gastritis, infiltration of M2 macrophages, and intestinalized SPEM

Since IL-33 blockade is effective in dampening both infiltration of CD163^{+} M2 macrophages, as well as intestinal-like metaplasia, but not recruitment of eosinophils in SAMP, we tested whether earlier intervention of eosinophil depletion has downstream effects on advanced, intestinalized SPEM. As such, 14-wk-old SAMP were treated with antibodies against CCR3 and IL-5, alone and in combination, previously shown to effectively deplete eosinophils[34,47,48]. Eosinophil depletion was confirmed in both peripheral BM and corpus tissues (**Figs. S7A** and **6A**, left panels), with histologic evaluation showing global improvement in restoring normal epithelial architecture,

reducing the presence of cellular immune infiltrates, and decreasing overall inflammation within the LP and hyperplasia of muscle wall layers in mice treated with anti-IL-5 and anti-CCR3, alone and in combination, vs. IgG-treated controls (**Figs. 6A, 6C**). Eosinophil depletion is also able to effectively decrease the presence of infiltrating IL-33-expressing M2 macrophages (**Figs. 6A, 6D** and **S7B**) and potently reduces gene expression of M2-associated molecules (**Fig. S7C**), but does not affect epithelial-derived IL-33 (**Fig. S7D)**. Importantly, CD44v co-labeling with GSII and GIF reveals that, while no dramatic differences are observed in GSII among experimental groups, increased intensity of GIF is noted, particularly in SAMP treated with either anti-IL-5 or combination anti-IL-5/anti-CCR3 vs. controls, indicating at least partial reversal of oxyntic atrophy (**Fig. 6A**, right panels). Interestingly, the decreased *Mist1* seen during SPEM is dramatically reversed following eosinophil depletion (**Fig. 6E**), suggesting eosinophil-dependent chief cell transdifferentiation during SPEM. Taken together, these results indicate an essential role for eosinophils in the development of intestinalized SPEM.

Discussion

Increasing evidence confirms the importance of the IL-33/ST2 axis in development of both gastritis and gastric cancer; in this context, IL-33 is an ideal candidate to link these two processes. However, while several studies report associative findings in patients, correlating increased IL-33 with intestinal-type gastric cancer[18] and poor prognostic factors[15,49], less is known regarding specific IL-33-dependent mechanisms leading to these pathologies. Based on the published literature and data from the present study, we propose a working hypothesis regarding the

mechanistic role of IL-33 in promoting SPEM progression and the gastritis-metaplasia-dysplasia-carcinoma sequelae, in which eosinophils play a central role.

SPEM/intestinalized SPEM is considered by some to be a mandatory step for dysplasia, and eventually carcinoma, to proceed[50]. Once established, intestinalized SPEM and/or intestinal metaplasia may not be reversible in the presence of inciting factors, such as chronic inflammation[51]. In fact, along with distinct gastric epithelial changes, an essential component to attain intestinal-like characteristics is non-resolving, chronic inflammation, often thought to be dependent on *H. pylori* status[51,52]. In this setting, IL-33 represents a critical mediator for SPEM/intestinalized SPEM to manifest, considering its ability to both potently stimulate epithelial proliferation and metaplasia, as well as induce and sustain chronic, Th2-driven inflammation.

Our data show that the most prevalent form of IL-33 in SAMP with established disease is bioactive fIL-33, which is released during chronic inflammation, with minimal presence of the less bioactive cleaved form (cIL-33)[38-40] that is more highly expressed in uninflamed AKR stomachs. In uninflamed young mice (AKR/SAMP) and older AKR, nuclear sequestration occurs within gastric epithelial cells, serving as reservoirs for IL-33 that is readily available for immediate release upon exposure to appropriate stimuli[18]. In fact, under homeostatic conditions, IL-33's primary role in the GI tract is believed to be epithelial repair and restitution, and to promote overall mucosal wound healing[33,53]. Interestingly, we found that, at the transcript level, *Il33* is significantly decreased in SAMP compared to AKR, which likely reflects a negative feedback mechanism in response to high systemic IL-33. In line with this finding, after exogenous IL-33 administration, *Il33* is also decreased, while the *Il1rl1* variant coding for sST2 (soluble

decoy receptor) is greatly increased, which together serves to downregulate overall IL-33 bioactivity.

The present study also introduces the SAMP mouse strain as a model of intestinalized SPEM that develops spontaneously and progresses in severity, without chemical, genetic or immunologic manipulation. These mice provide an ideal tool to investigate the natural course of disease and a convenient system to test potential pre-clinical therapies for pre-neoplastic conditions that may lead to gastric cancer, in which both preventive and therapeutic strategies can be effectively implemented. Using a therapeutic approach, we found that IL-33 neutralization by sST2-Fc administration is effective at reversing intestinalized SPEM, primarily by targeting the epithelial compartment and reducing IL-33-dependent epithelial alterations, which are hallmark features of metaplasia. In addition, IL-33 blockade decreases severity of chronic gastritis and the presence of M2 macrophages, which are also characteristic of metaplasia and progression to intestinalized SPEM[31]. Importantly, using SAMP, we not only demonstrate the essential role for IL-33 in the development of intestinal-like metaplasia, but that the IL-33/ST2 axis is important for several steps throughout this process. For example, IL-33 clearly has direct effects on epithelial cells. Indeed, epithelial alterations within the GI tract were among the initial aberrancies described after healthy mice were exposed to high levels of IL-33[9]. We and others[41] confirmed these observations in the stomach, showing that rIL-33 induces severe oxyntic atrophy and upregulates specific markers of SPEM. Alternatively, IL-33 also has profound effects on the gastric immune compartment, promoting, for example, vigorous infiltration of eosinophils and M2 macrophages[31], further perpetuating a chronic inflammatory

state. Importantly, prolonged and elevated levels of IL-33 has the ability to sustain chronic inflammation in the stomach, which is essential for intestinal metaplasia to advance to gastric cancer.

The results of our study also underscore the importance of eosinophils in the development of intestinal-like metaplasia, and that IL-33 plays a critical role in the systemic expansion and early recruitment of eosinophils into the gastric mucosa of SAMP, as well as AKRs treated with rIL-33. Previously, eosinophils in gastric metaplasia and cancer development have been proposed to have both pathogenic as well as protective functions. A prior study investigating early gastric cancers demonstrated the presence of tumor stromal eosinophils with morphologic evidence of activation, as well as tumor cells in intimate contact with activated eosinophils with focal cytopathic changes[54]. Gastric carcinomas have also been reported to express eosinophil-associated chemotactic cytokines, including IL-2, IL-5 and GM–CSF, with expression of GM–CSF appearing to be specific for signet ring carcinoma cells[55]. On the other hand, in support of a protective function, high pre-operative eosinophil counts were found to correlate with prolonged survival after surgery[56], and the -28G polymorphism in the promoter region of the eosinophil chemoattractant, RANTES, is associated with a reduced risk of developing severe intestinal metaplasia[57].

Nonetheless, while our results indicate that eosinophils play an important role during early events leading to gastritis/metaplasia, one can certainly speculate that other IL-33-responsive innate immune cell populations may also contribute. Our data show that IL-33 can promote local recruitment of M2 macrophages that themselves, are potent producers of IL-33. These findings are in line with previous reports demonstrating

the ability of IL-33 to increase overall macrophage numbers in the stomach and to polarize them to an alternatively-activated M2 phenotype, albeit in the periphery (peritoneum)[41], and that M2 macrophages are dramatically reduced in IL-33-deficient mice in which advanced SPEM has been elicited, but that can also be rescued by administering rIL-13[31]. Our findings in SAMP, however, indicate that M2 macrophage infiltration is likely downstream of eosinophil activation and recruitment since eosinophil depletion, similar to systemic IL-33 blockade, has a significant impact on reducing the infiltration of gastric M2 macrophages that also happen to produce IL-33. Interestingly, however, eosinophil depletion does not appear to have an effect on IL-33 expression in the gastric epithelium of SAMP. In contrast, L635-induced SPEM does not appear to require eosinophils[31], which may simply reflect differences in inciting factors between the two models, *i.e*., chemical obliteration of parietal cells vs. chronic, non-resolving inflammation. An alternative hypothesis is that ILC2s are also an IL-33-responsive innate immune cell population that can affect SPEM. ILC2s have not been detected and/or isolated from gastric tissues until recently, when Li *et al*. reported the prevalence of GATA-3^{+}Lin^{-} cells in tumors of patients with *H. pylori*-associated gastric cancer[58]. Of note, and counter-intuitive to this finding, Buzzelli *et al*., showed that IL-33 is rapidly induced after acute *H. pylori* infection, but suppressed in chronic infection[41]. However, in the former study, it is unclear what the IL-33 levels were, if they correlated with GATA-3^{+}Lin^{-} ILC2 frequency, and if IL-33 exhibited temporal changes during early vs. late stages in different types of gastric cancers. In the latter study, acute vs. chronic *H. pylori* infection is defined as 1 and 7 days vs. 2 months, which may not reflect chronic infection, especially in gastric cancer-susceptible individuals. Although indirect evidence

suggests emergence of gastric ILC2s in IL-33-treated mice[41], we recently reported increased ILC2s after L635-dependent acute gastric injury[59]. Similarly, in SAMP mice, preliminary data also show an increased frequency, albeit quite low, of ILC2s vs. AKR (**Fig. S8**); however, whether ILC2s contribute to the SAMP gastric phenotype is unknown. Based on studies characterizing SAMP lacking T/B cells, but with intact ILC function (*i.e.*, SAMPx*Rag2*$^{-/-}$ strain), ILCs likely play a negligible role in SPEM development since these mice, without the ability to mount adaptive immune responses and sustain a chronic inflammatory state, have virtually normal stomachs (**Fig. S8**). Finally, yet another IL-33-responsive innate immune cell population (*i.e.*, mast cells) has been recently implicated in the development of gastric cancer in *gp130*$^{F/F}$ mice, specifically through mobilization of macrophages[18]. While similar to early, IL-33-dependent activation of eosinophils upstream of macrophage recruitment, it is unclear as to the precise temporal involvement of mast cells, and their interaction(s) with other mucosal populations to promote events leading to intestinal metaplasia and gastric cancer.

Taken together, the present study underscores a critical role for IL-33 in the development of chronic inflammation and metaplasia in the stomach, and implicates eosinophils as an early, IL-33-responsive innate immune cell population that participates in the complex orchestration leading to SPEM/intestinalized SPEM. As such, targeting the IL-33/ST2 axis for future therapeutic modalities to interrupt the early, initial events leading to gastritis and metaplasia, and potentially reversing intestinalizing SPEM, may prove to be beneficial for the prevention and/or treatment of patients susceptible to gastric cancer.

References

1. Balkwill F, Mantovani A. Inflammation and cancer: back to Virchow? Lancet 2001;357:539-45.
2. Crusz SM, Balkwill FR. Inflammation and cancer: advances and new agents. Nat Rev Clin Oncol 2015;12:584-96.
3. Mantovani A, Barajon I, Garlanda C. IL-1 and IL-1 regulatory pathways in cancer progression and therapy. Immunol Rev 2018;281:57-61.
4. Lopetuso LR, Chowdhry S, Pizarro TT. Opposing functions of classic and novel IL-1 family members in gut health and disease. Front Immunol 2013;4:181.
5. Maywald RL, Doerner SK, Pastorelli L, et al. IL-33 activates tumor stroma to promote intestinal polyposis. Proc Natl Acad Sci USA 2015;112:E2487-96.
6. Malik A, Sharma D, Zhu Q, et al. IL-33 regulates the IgA-microbiota axis to restrain IL-1alpha-dependent colitis and tumorigenesis. J Clin Invest 2016;126:4469-4481.
7. **He Z**, **Chen L**, Souto FO, et al. Epithelial-derived IL-33 promotes intestinal tumorigenesis in Apc(Min/+) mice. Sci Rep 2017;7:5520.
8. Venerito M, Nardone G, Selgrad M, et al. Gastric cancer-epidemiologic and clinical aspects. Helicobacter 2014;19 Suppl 1:32-7.
9. Schmitz J, Owyang A, Oldham E, et al. IL-33, an interleukin-1-like cytokine that signals via the IL-1 receptor-related protein ST2 and induces T helper type 2-associated cytokines. Immunity 2005;23:479-90.
10. Pastorelli L, Garg RR, Hoang SB, et al. Epithelial-derived IL-33 and its receptor ST2 are dysregulated in ulcerative colitis and in experimental Th1/Th2 driven enteritis. Proc Natl Acad Sci USA 2010;107:8017-22.
11. **Neill DR**, **Wong SH**, **Bellosi A**, et al. Nuocytes represent a new innate effector leukocyte that mediates type-2 immunity. Nature 2010;464:1367-70.
12. Joshi AD, Oak SR, Hartigan AJ, et al. Interleukin-33 contributes to both M1 and M2 chemokine marker expression in human macrophages. BMC Immunology 2010;11.
13. Stolarski B, Kurowska-Stolarska M, Kewin P, et al. IL-33 exacerbates eosinophil-mediated airway inflammation. J Immunol 2010;185:3472-80.
14. **Hung LY**, **Lewkowich IP**, Dawson LA, et al. IL-33 drives biphasic IL-13 production for noncanonical Type 2 immunity against hookworms. Proc Natl Acad Sci USA 2013;110:282-7.
15. **Sun P**, **Ben Q**, Tu S, et al. Serum interleukin-33 levels in patients with gastric cancer. Dig Dis Sci 2011;56:3596-601.
16. Ye XL, Zhao YR, Weng GB, et al. IL-33-induced JNK pathway activation confers gastric cancer chemotherapy resistance. Oncol Rep 2015;33:2746-52.
17. Yu XX, Hu Z, Shen X, et al. IL-33 promotes gastric cancer cell invasion and migration via ST2-ERK1/2 pathway. Dig Dis Sci 2015;60:1265-72.
18. Eissmann MF, Dijkstra C, Jarnicki A, et al. IL-33-mediated mast cell activation promotes gastric cancer through macrophage mobilization. Nat Commun 2019;10:2735.
19. Correa P. A human model of gastric carcinogenesis. Cancer Res 1988;48:3554-60.
20. Saenz JB, Mills JC. Acid and the basis for cellular plasticity and reprogramming in gastric repair and cancer. Nat Rev Gastroenterol Hepatol 2018;15:257-273.
21. Goldenring JR. Pyloric metaplasia, pseudopyloric metaplasia, ulcer-associated cell lineage and spasmolytic polypeptide-expressing metaplasia: reparative lineages in the gastrointestinal mucosa. J Pathol 2018;245:132-137.
22. Schmidt PH, Lee JR, Joshi V, et al. Identification of a metaplastic cell lineage associated with human gastric adenocarcinoma. Lab Invest 1999;79:639-46.

23. **Nam KT**, **Lee HJ,** Sousa JF, et al. Mature chief cells are cryptic progenitors for metaplasia in the stomach. Gastroenterology 2010;139:2028-2037.
24. Mills JC, Sansom OJ. Reserve stem cells: Differentiated cells reprogram to fuel repair, metaplasia, and neoplasia in the adult gastrointestinal tract. Sci Signal 2015;8:re8.
25. Radyk MD, Burclaff J, Willet SG, et al. Metaplastic cells in the stomach arise, independently of stem cells, via dedifferentiation or transdifferentiation of chief cells. Gastroenterology 2018;154:839-843.
26. Lennerz JK, Kim SH, Oates EL, et al. The transcription factor MIST1 is a novel human gastric chief cell marker whose expression is lost in metaplasia, dysplasia, and carcinoma. Am J Pathol 2010;177:1514-33.
27. Burclaff J, Osaki LH, Liu D, et al. Targeted apoptosis of parietal cells is insufficient to induce metaplasia in stomach. Gastroenterology 2017;152:762-766.
28. **Willet SG**, **Lewis MA**, **Miao ZF**, et al. Regenerative proliferation of differentiated cells by mTORC1-dependent paligenosis. EMBO J 2018;37.
29. Weis VG, Sousa JF, LaFleur BJ, et al. Heterogeneity in mouse spasmolytic polypeptide-expressing metaplasia lineages identifies markers of metaplastic progression. Gut 2013;62:1270-9.
30. Petersen CP, Weis VG, Nam KT, et al. Macrophages promote progression of spasmolytic polypeptide-expressing metaplasia after acute loss of parietal cells. Gastroenterology 2014;146:1727-38.
31. Petersen CP, Meyer AR, De Salvo C, et al. A signalling cascade of IL-33 to IL-13 regulates metaplasia in the mouse stomach. Gut 2018;67:805-817.
32. Reuter BK, Pastorelli L, Brogi M, et al. Spontaneous, immune-mediated gastric inflammation in SAMP1/YitFc mice, a model of Crohn's-like gastritis. Gastroenterology 2011;141:1709-19.
33. Lopetuso LR, De Salvo C, Pastorelli L, et al. IL-33 promotes recovery from acute colitis by inducing miR-320 to stimulate epithelial restitution and repair. Proc Natl Acad Sci USA 2018;115:E9362-E9370.
34. De Salvo C, Wang XM, Pastorelli L, et al. IL-33 drives eosinophil infiltration and pathogenic type 2 helper T-cell immune responses leading to chronic experimental ileitis. Am J Pathol 2016;186:885-98.
35. Arseneau KKO, Cominelli F. Improving the reproducibility and quality of reporting for animal studies in inflammatory bowel disease. Inflamm Bowel Dis 2017;23:2069-2071.
36. Turani H, Lurie B, Chaimoff C, et al. The diagnostic significance of sulfated acid mucin content in gastric intestinal metaplasia with early gastric cancer. Am J Gastroenterol 1986;81:343-5.
37. Nozaki K, Ogawa M, Williams JA, et al. A molecular signature of gastric metaplasia arising in response to acute parietal cell loss. Gastroenterology 2008;134:511-22.
38. Talabot-Ayer D, Lamacchia C, Gabay C, et al. Interleukin-33 is biologically active independently of caspase-1 cleavage. J Biol Chem 2009;284:19420-6.
39. Cayrol C, Girard JP. The IL-1-like cytokine IL-33 is inactivated after maturation by caspase-1. Proc Natl Acad Sci USA 2009;106:9021-6.
40. **Luthi AU**, **Cullen SP**, McNeela EA, et al. Suppression of interleukin-33 bioactivity through proteolysis by apoptotic caspases. Immunity 2009;31:84-98.
41. Buzzelli JN, Chalinor HV, Pavlic DI, et al. IL33 Is a stomach alarmin that initiates a skewed Th2 response to injury and infection. Cell Mol Gastroenterol Hepatol 2015;1:203-221.
42. **Wada T**, **Ishimoto T,** Seishima R, et al. Functional role of CD44v-xCT system in the development of spasmolytic polypeptide-expressing metaplasia. Cancer Sci 2013;104:1323-9.
43. Fagundes CT, Amaral FA, Souza AL, et al. ST2, an IL-1R family member, attenuates inflammation and lethality after intestinal ischemia and reperfusion. J Leukoc Biol 2007;81:492-9.

44. Miao ZF, Adkins-Threats M, Burclaff JR, et al. A metformin-responsive metabolic pathway controls distinct steps in gastric progenitor fate decisions and maturation. Cell Stem Cell 2020;26:910-925.
45. Mishra A, Hogan SP, Lee JJ, et al. Fundamental signals that regulate eosinophil homing to the gastrointestinal tract. J Clin Invest 1999;103:1719-27.
46. Hogan SP, Rosenberg HF, Moqbel R, et al. Eosinophils: biological properties and role in health and disease. Clin Exp Allergy 2008;38:709-50.
47. Masterson JC, McNamee EN, Jedlicka P, et al. CCR3 blockade attenuates eosinophilic ileitis and associated remodeling. Am J Pathol 2011;179:2302-14.
48. Song DJ, Shim MH, Lee N, et al. CCR3 monoclonal antibody inhibits eosinophilic inflammation and mucosal injury in a mouse model of eosinophilic gastroenteritis. Allergy Asthma Immunol Res 2017;9:360-367.
49. Hu W, Li X, Li Q, et al. Interleukin-33 expression does not correlate with survival of gastric cancer patients. Pathol Oncol Res 2017;23:615-619.
50. Fox JG, Wang TC. Inflammation, atrophy, and gastric cancer. J Clin Invest 2007;117:60-9.
51. Correa P, Piazuelo MB. The gastric precancerous cascade. J Dig Dis 2012;13:2-9.
52. Petersen CP, Mills JC, Goldenring JR. Murine models of gastric corpus preneoplasia. Cell Mol Gastroenterol Hepatol 2017;3:11-26.
53. Monticelli LA, Osborne LC, Noti M, et al. IL-33 promotes an innate immune pathway of intestinal tissue protection dependent on amphiregulin-EGFR interactions. Proc Natl Acad Sci USA 2015;112:10762-7.
54. Caruso RA, Giuffre G, Inferrera C. Minute and small early gastric carcinoma with special reference to eosinophil infiltration. Histol Histopathol 1993;8:155-66.
55. Hong SW, Cho MY, Park C. Expression of eosinophil chemotactic factors in stomach cancer. Yonsei Med J 1999;40:131-6.
56. Iwasaki K, Torisu M, Fujimura T. Malignant tumor and eosinophils. I. Prognostic significance in gastric cancer. Cancer 1986;58:1321-7.
57. Tahara T, Arisawa T, Shibata T, et al. Effect of RANTES promoter genotype on the severity of intestinal metaplasia in Helicobacter pylori-infected Japanese subjects. Dig Dis Sci 2009;54:1247-52.
58. Li R, Jiang XX, Zhang LF, et al. Group 2 innate lymphoid cells are involved in skewed type 2 immunity of gastric diseases induced by Helicobacter pylori infection. Mediators Inflamm 2017;2017:4927964.
59. Meyer AR, Engevik AC Madorsky T, et al. Group 2 innate lymphoid cells coordinate damage response in the stomach. Gastroenterology 2020;in press.

Figure Legends

Figure 1. *Differential IL-33 localization/expression in corpus of gastritis-prone SAMP vs. control AKR*. *(A)* Representative IHC images localizing IL-33 prior to inflammation (4-wk-old) and during established disease (20-wk-old) in SAMP (N=8). Original magnification: X10+2.0, X40+2.0 (*insets*); scale bars: 100μm, 50μm (*insets*). *(B)* Representative Western blot differentiating bioactive full-length (f)- from cleaved (c)-IL-33 (N=4). *(C) Il33* expressed as fold-change vs. age-matched AKR, **P*<0.05, ****P*<0.001 (N=7-8). *(D)* IF co-localization of IL-33 (red) and CD163 (green) show abundance of IL-33-producing M2 macrophages (yellow), further augmented after rIL-33 in AKR (N=4), and *(E)* confirmed by FACS, **P*<0.01 (N=6). Original magnification: X20; scale bars: 10μm, 5μm (*insets*).

Figure 2. *IL-33 administration to healthy AKR induces striking gastric mucosal alterations*. *(A)* Representative photos of bisected stomachs, highlighting presence of gastric mucosal folds (*black arrows*), and photomicrographs of corpus, displaying parietal cell (*white arrowheads*) atrophy, loss of chief cell (*white arrows*) differentiation, hyperproliferation of mucus-producing cells (*black arrows*), and active proliferation of $BrdU^+$ mucous neck cells after rIL-33; original magnification: X10, X40 (*insets*); scale bars: 100μm, 50μm (*insets*). *(B)* Gastric inflammation, epithelial hyperplasia, and *(C)* representative photomicrographs showing appearance of acidic mucins by Alcian blue/PAS-staining (*arrows*; parietal cells indicated by *arrowheads*), and increased presence/intensity of GSII lectin (green) and Cd44v (red) after rIL-33; original magnification (left-to-right): X20+1.25, X40+1.25, X20, X40 (*insets*); scale bars: 100μm,

50μm (*insets*). *(D)* Semi-quantitative assessment of SPEM. ***P*<0.01, *****P*<0.0001 (N=13-16).

Figure 3. *Molecular profiling indicates overt metaplasia in AKR corpus after acute exposure to IL-33.* Relative transcript levels of *(A) Gif*, *Atp4a*, *Tff1*, *Tff2, (B) He4*, *Clu*, *(C) Cftr*, *Dmbt1*, *Etv5*, *(D) Il33,* and *Il1rl1* variant 1 (ST2L) and 2 (sST2) after rIL-33. Data expressed as fold-change vs. vehicle controls; **P*<0.05, ***P*<0.01, ****P*<0.001 (N=8).

Figure 4. *Neutralization of IL-33 attenuates chronic gastritis and intestinalized SPEM in SAMP. (A)* Representative photomicrographs of H&E-, Alcian blue/PAS-, and DBA-stained corpus after sST2-Fc (*left panels*). While IF for GIF (blue) remains relatively unchanged, CD44v (green) and GSII-lectin (red/blue) are decreased, and IL-33 (red)/CD163 (green) show marked reduction of IL-33-producing M2 macrophages (yellow) after sST2-Fc (*right panels*). Original magnification: X20+1.25. *(B)* Parietal cell numbers (*arrows*, panel A), *(C)* epithelial hyperplasia, and *(D)* gastric inflammation after sST2-Fc; **P*<0.05, ***P*<0.01 (N=9-11).

Figure 5. *Early IL-33-dependent peripheral expansion and increased eosinophil recruitment to SAMP stomachs. (A)* Percentages of BM-derived eosinophils (EOS), and representative IHC photomicrographs of corpus from *(B)* SAMP vs. AKR, *(C)* SAMPx*Il33*$^{-/-}$ vs. WT littermates, *(D)* IL-33- vs. vehicle-treated AKR, and *(E)* sST2-Fc- vs. IgG-treated SAMP, stained for MBP and eosinophil counts. Original magnification: X10+1.25; scale bars: 100μm. ***P*<0.01, ****P*<0.001 (N=4-10).

Figure 6. *Eosinophil depletion reduces gastritis, M2 macrophage recruitment and SPEM in SAMP. (A)* Representative photomicrographs of corpus stained (left-to right): for MBP (eosinophils), with H&E, and by IF for IL-33- (red) expressing $CD163^+$ (green) M2 macrophages (yellow), showing reduction after anti-IL-5, anti-CCR3 or combination anti-IL-5/CCR3, and for GSII (green), CD44v (red) and GIF (blue) showing specific increase in GIF (*arrowheads*), suggesting protection from oxyntic atrophy. Original magnification: X20, X40 (*insets*); scale bars: 100μm, 50μm (*insets*). Quantitation of gastric *(B)* eosinophils, *(C)* inflammation, *(D)* IL-33-expressing M2 macrophages, and *(E) Mist1* after eosinophil depletion; **P*<0.05. Data representative of 3 experiments (N=7-8/expt).

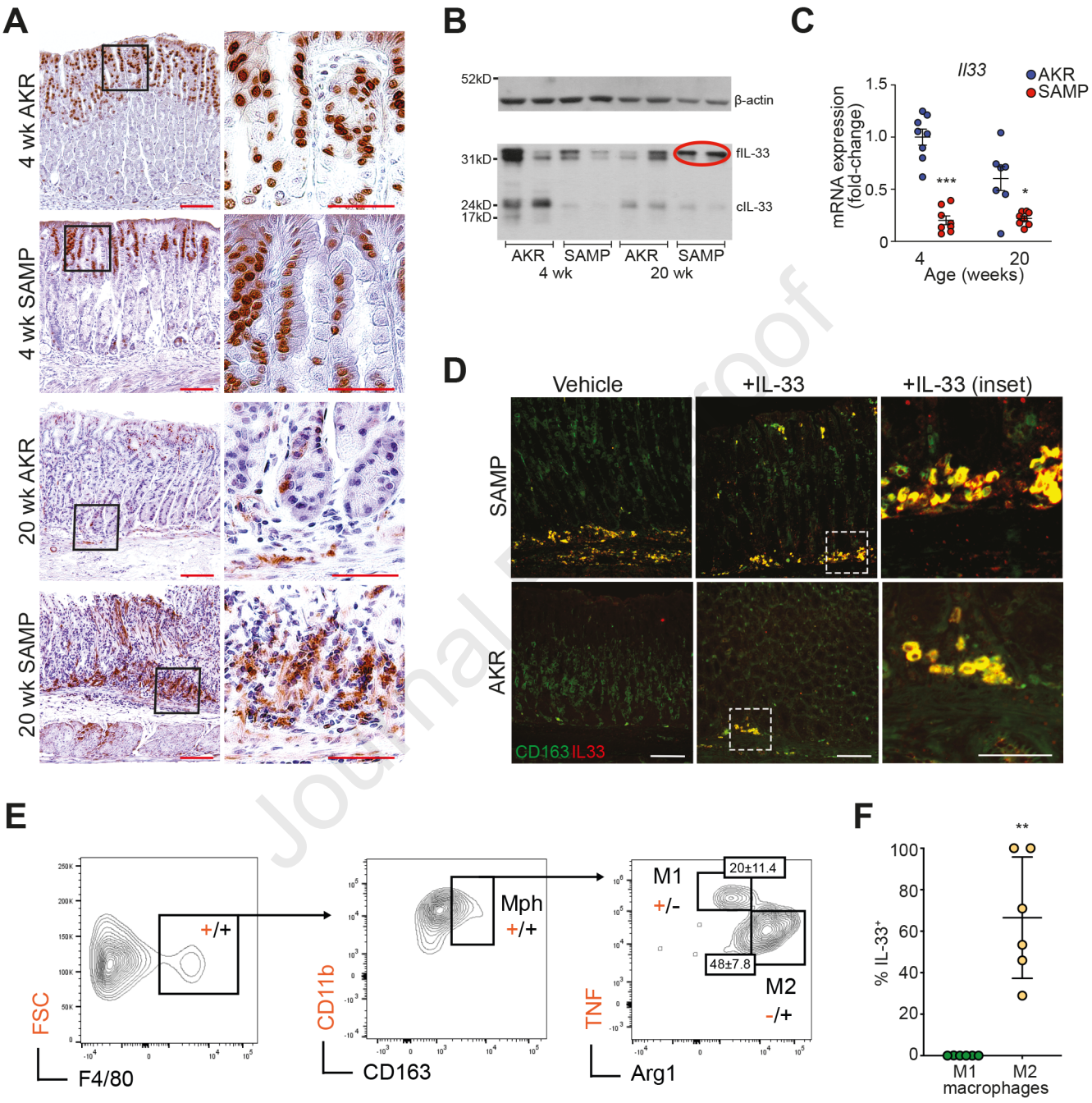
A
4 wk AKR
4 wk SAMP
20 wk AKR
20 wk SAMP
B
52kD
β-actin
31kD
fIL-33
24kD
17kD
cIL-33
AKR
SAMP
AKR
SAMP
4 wk
20 wk
C
Il33
AKR
SAMP
mRNA expression (fold-change)
1.5
1.0
0.5
0
***
*
4
20
Age (weeks)
D
Vehicle
+IL-33
+IL-33 (inset)
SAMP
AKR
CD163 IL33
E
FSC
+/+
F4/80
CD11b
Mph
+/+
CD163
TNF
M1
+/-
20±11.4
48±7.8
M2
-/+
Arg1
F
**
100
80
60
40
20
0
% IL-33+
M1
M2
macrophages

Figure 1

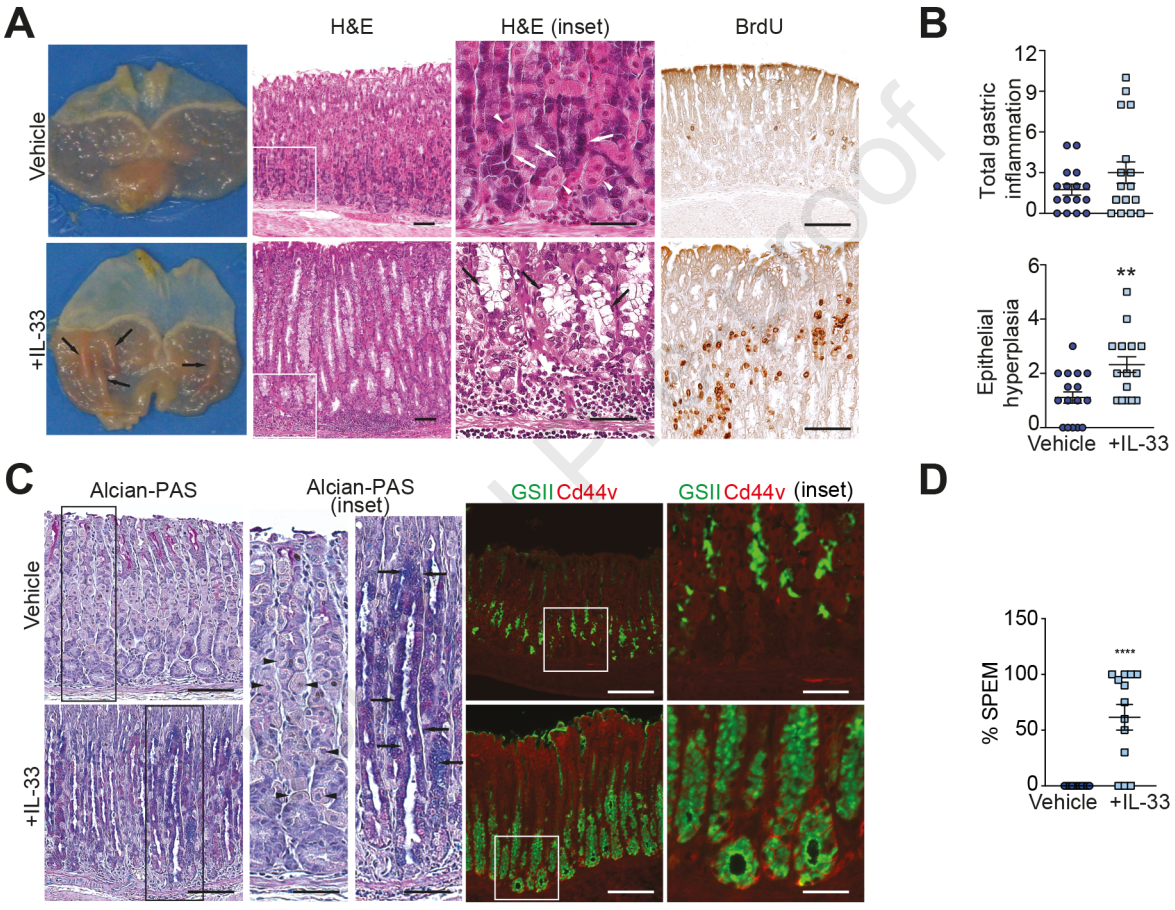
A
H&E
H&E (inset)
BrdU
Vehicle
+IL-33
B
Total gastric inflammation
12
9
6
3
0
Epithelial hyperplasia
6
4
2
0
**
Vehicle
+IL-33
C
Alcian-PAS
Alcian-PAS (inset)
GSII Cd44v
GSII Cd44v (inset)
Vehicle
+IL-33
D
% SPEM
150
100
50
0
****
Vehicle
+IL-33

Figure 2

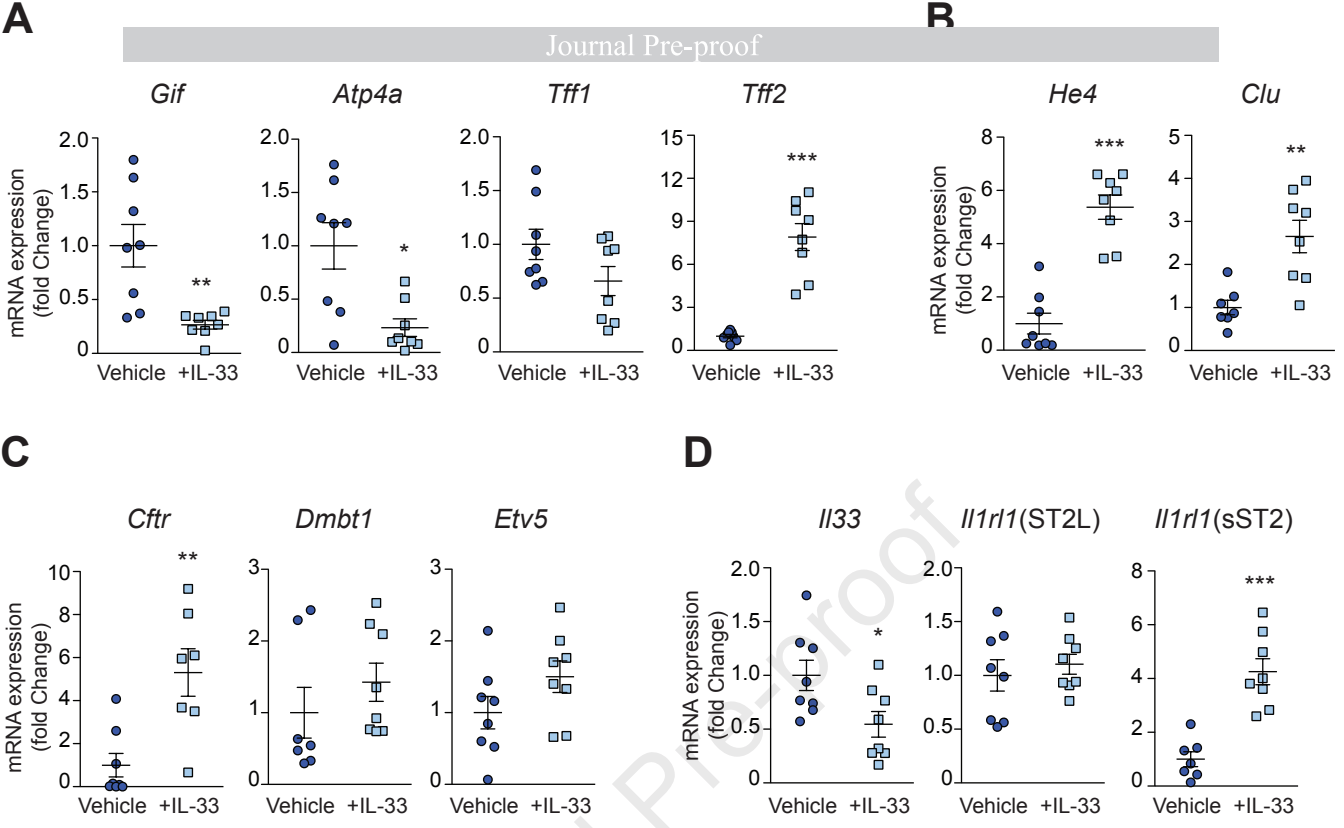

Figure 3

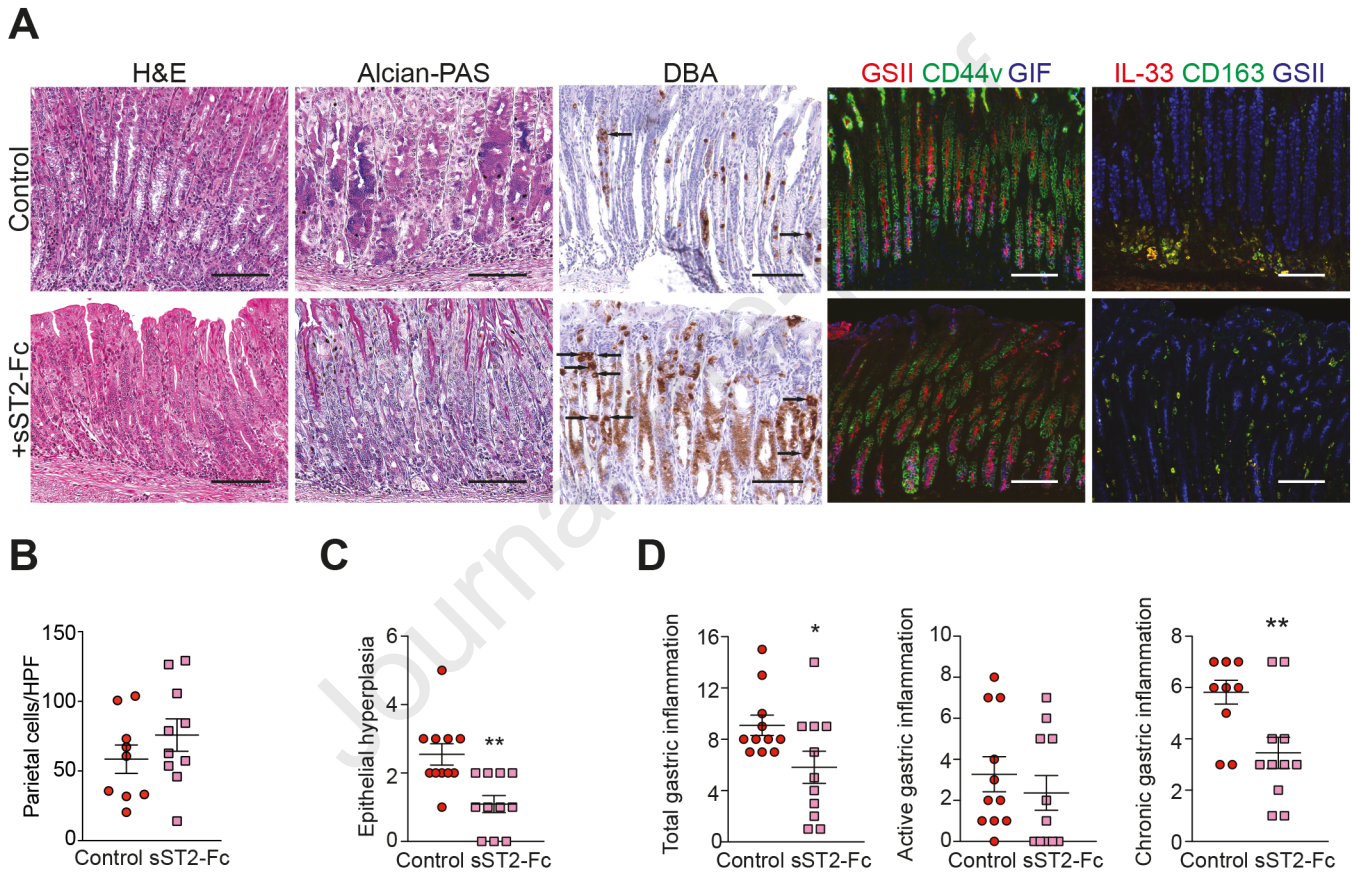
A
H&E
Alcian-PAS
DBA
GSII CD44v GIF
IL-33 CD163 GSII
Control
+sST2-Fc
B
Parietal cells/HPF
150
100
50
0
Control sST2-Fc
C
Epithelial hyperplasia
6
4
2
0
**
Control sST2-Fc
D
Total gastric inflammation
16
12
8
4
0
*
Control sST2-Fc
Active gastric inflammation
10
8
6
4
2
0
Control sST2-Fc
Chronic gastric inflammation
8
6
4
2
0
**
Control sST2-Fc

Figure 4

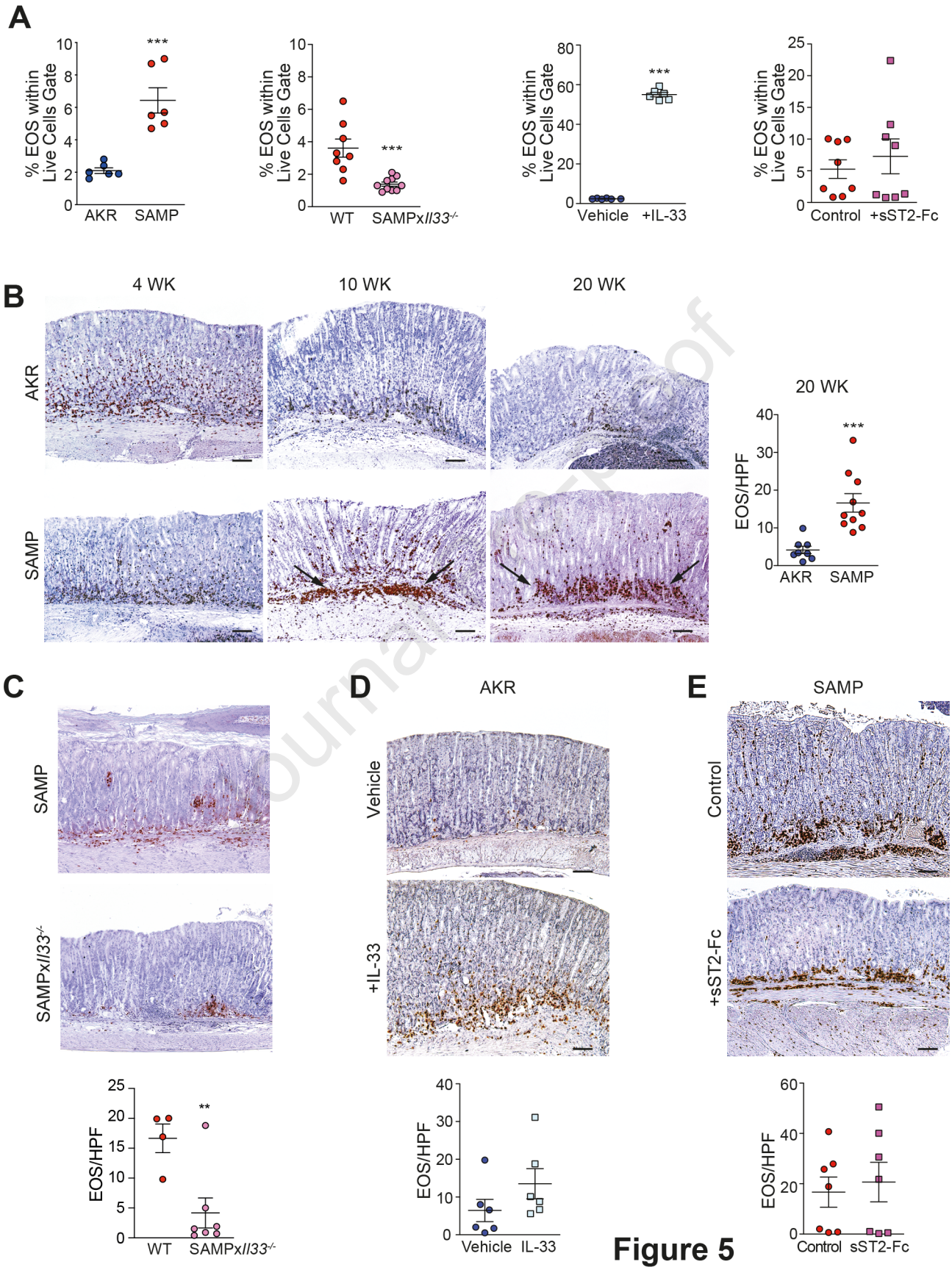

Figure 5

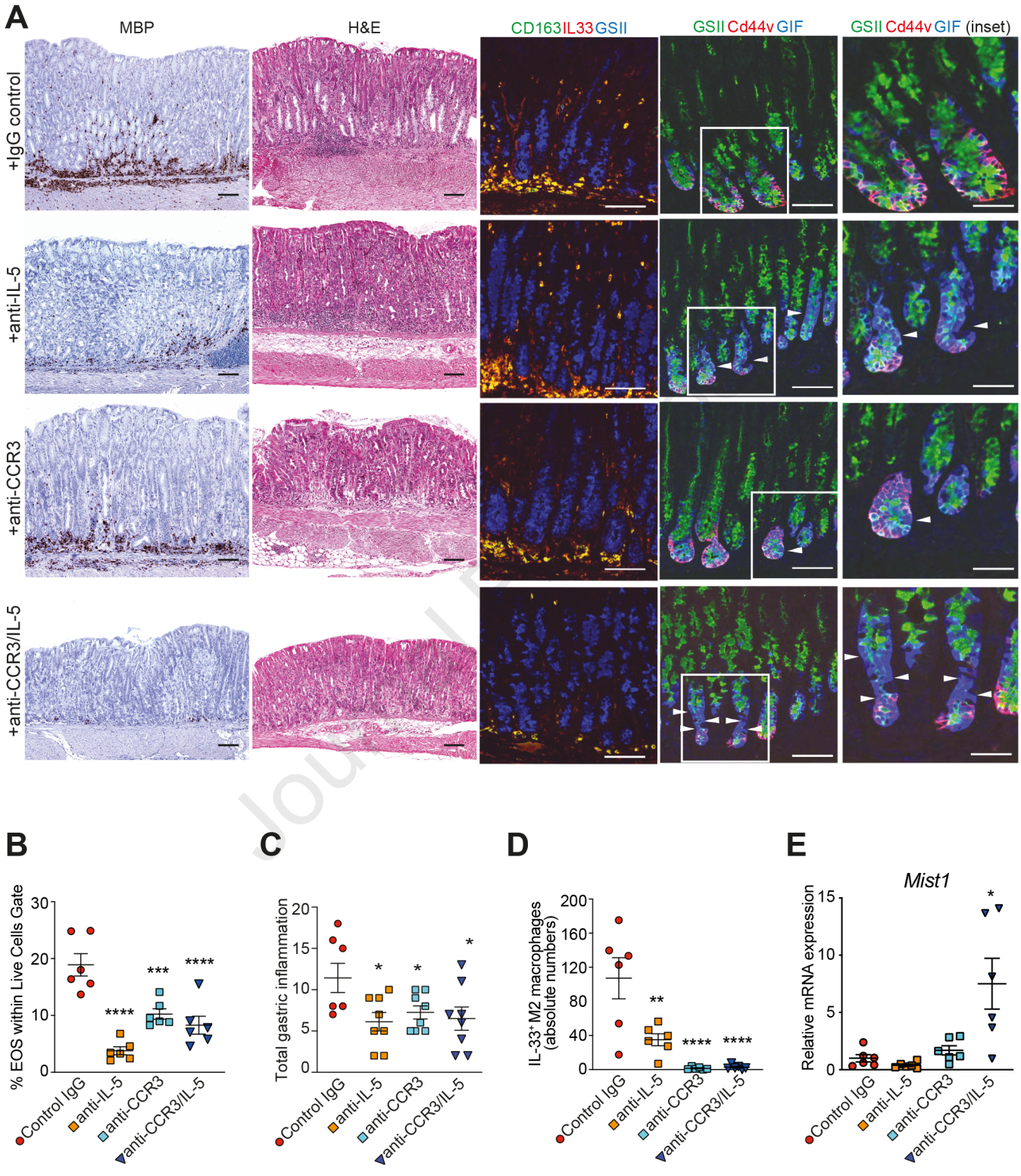
A
MBP
H&E
CD163IL33GSII
GSII Cd44v GIF
GSII Cd44v GIF (inset)
+IgG control
+anti-IL-5
+anti-CCR3
+anti-CCR3/IL-5
B
% EOS within Live Cells Gate
C
Total gastric inflammation
D
IL-33+ M2 macrophages (absolute numbers)
E
Mist1
Relative mRNA expression
Control IgG
anti-IL-5
anti-CCR3
anti-CCR3/IL-5

Figure 6

Supplemental Figure Legends

Figure S1. *Evidence of advanced intestinalized SPEM in stomachs of gastritis-prone SAMP mice*. *(A)* Representative histologic image of 4-wk-old SAMP shows early hyperproliferation of gastric glands compared to age-matched AKR (*left panels*), while in 20-wk-old SAMP, Alcian blue/PAS staining highlights acidic mucin-secreting cells (a*rrows*) replacing parietal (*arrowheads*) and chief cells as SPEM progresses, which is absent in age-matched AKR (*right panels*). Original magnification: X20+1.25; scale bars: 100μm (N=6-8). (*B*) Representative IF images of full-thickness corpus from 4-wk-old SAMP display early, aberrant staining of GSII (green) and Clu (red), characteristic of SPEM (*left lower panels*) compared to age-matched AKR (*left upper panels*) that becomes more evident in 20-wk-old SAMP with established gastritis, with clear abundance of $GSII^+$ cells and increased CD44v and Clu (both red), localizing to base of gastric glands (*arrows*, *right lower panels*) when compared to age-matched AKR controls (*right upper panels*). Original magnification: X20; scale bars: 100μm.

Figure S2. *Molecular profiling indicates advanced SPEM in SAMP corpus that progresses with age.* Relative expression of *(A) Gif*, *Atp4a*, *Tff1*, *(B) Tff2, Mist1*, *(C) He4*, *Clu*, *Lyz*, *Gpx2*, and *(D) Cftr*, *Dmbt1*, *Etv5* in young SAMP vs. SAMP with established disease and vs. age-matched AKR controls. Data is expressed as fold-change vs. 4-wk-old AKR (with mean arbitrarily set as 1); **P*<0.05, ***P*<0.01, ****P*<0.001 vs. age-matched AKR, and $^{\#\#}P$<0.01, $^{\#\#\#}P$<0.001 vs. 4-wk-old AKR/SAMP (N=6-9).

Figure S3. *Increased circulating levels of IL-33 in SAMP mice*. Serum levels of total IL-33 protein in 4-, 10- and 20-wk-old SAMP vs. age-matched control AKR; **P*<0.05, ****P*<0.001 vs. age-matched AKR. $^{\#}$*P*<0.05 vs. 4-wk-old SAMP (N=3-6).

Figure S4. *Gating strategy for distinguishing M1 vs. M2 macrophages by flow cytometry.* Representative 2D dot plots (shown here for BM) for SAMP depict, from left to right: 1) SSC vs. FSC (gating on general cells), 2) FSC-A vs. FSC-H (gating on singlets), 3) SSC-A vs. live/dead (gating on live cells), 4) CD11b vs. SSC-A (gating on granulocytes), 5) Ly6G vs. SSC-A (gating on Ly6G^{-} cells), 6) CD163 vs. F4/80 (gating on macrophages, Mph), 7) TNF vs. MHCII (gating on M1 macrophages), and Arg1 vs. CD163 (gating on M2 macrophages).

Figure S5. *Strong prominence of M2- vs. M1-associated gene markers expressed in macrophages from SAMP vs. AKR mice.* Relative transcript levels of M1- vs. M2-associated molecules (defined in Sica and Mantovani, Trends Immunol 2002 and Murray, Immunity 2017) in isolated macrophages from 10-wk-old SAMP, normalized by *36B4* and expressed as % fold-change of age-matched AKR controls. Data is presented as mean±SD (N=6).

Figure S6. *Gating strategy for detecting eosinophils by flow cytometry*. Representative 2D dot plots (shown here for BM) for control AKR depict, from left to right: 1) SSC vs. FSC (P1, gating on general cells), 2) FSC-A vs. FSC-H (P2, gating on singlets), 3) SSC-A vs. live/dead (gating on live cells), and 4) CD11b vs. Siglec-F (gating on EOS).

Figure S7. *Eosinophil depletion is effective in decreasing peripheral (BM) and local (gastric) eosinophils, and reduces M2 macrophages and expression of M2-associated genes in SAMP stomachs. (A)* Frequency of peripheral (BM)-derived eosinophils (*left panel*) and eosinophil count (*right panel*), *(B)* M2 macrophage frequency (*left panel*), and M2 macrophage count (*right panel*, defined as IL-33^{+}CD163^{+} cells shown in **Fig. 6A**, middle panels) in SAMP corpus after eosinophil depletion by administration of anti-IL-5 and anti-CCR3, alone and in combination, vs. IgG-treated controls (N=4-9). *(C)* Relative transcript levels of M2-associated molecules, normalized by *36B4* and expressed as fold-change vs. IgG-treated controls (with mean set arbitrarily as 1) (N=6), and *(D)* representative IHC images localizing IL-33 (N=4). Original magnification: X10+1.25; scale bars: 100μm. **P*<0.05, ***P*<0.01, ****P*<0.001, *****P*<0.0001.

Figure S8. *Evidence that aberrant adaptive immune responses, and not increased ILC2 frequency, is essential for development of gastritis/SPEM in SAMP mice.* Corpus tissues were excised from stomachs of SAMP and AKR, processed into single-cell suspensions for flow cytometric analysis of ILC2s using the following gating strategy: (*A*) live cells were gated on CD45^{+}, then on CD127^{+} cells negative for lineage markers CD3 (T cells), CD11c (DCs), B220 (B cells), CD11b (myeloid cells), Ly6g, Ter-119 (granulocytes), and positive for the transcription factor, GATA3, (*B*) with ILC2s reported as both percentages and absolute numbers; **P*<0.05, ***P*<0.01 (N=3-7). (C) Epithelial hyperplasia (*left panels*) and total inflammation (*right panels*) in corpus from SAMP x RAG2$^{-/-}$ mice vs. WT controls; **P*<0.05, ***P*<0.01, ****P*<0.001 (N=7-15).

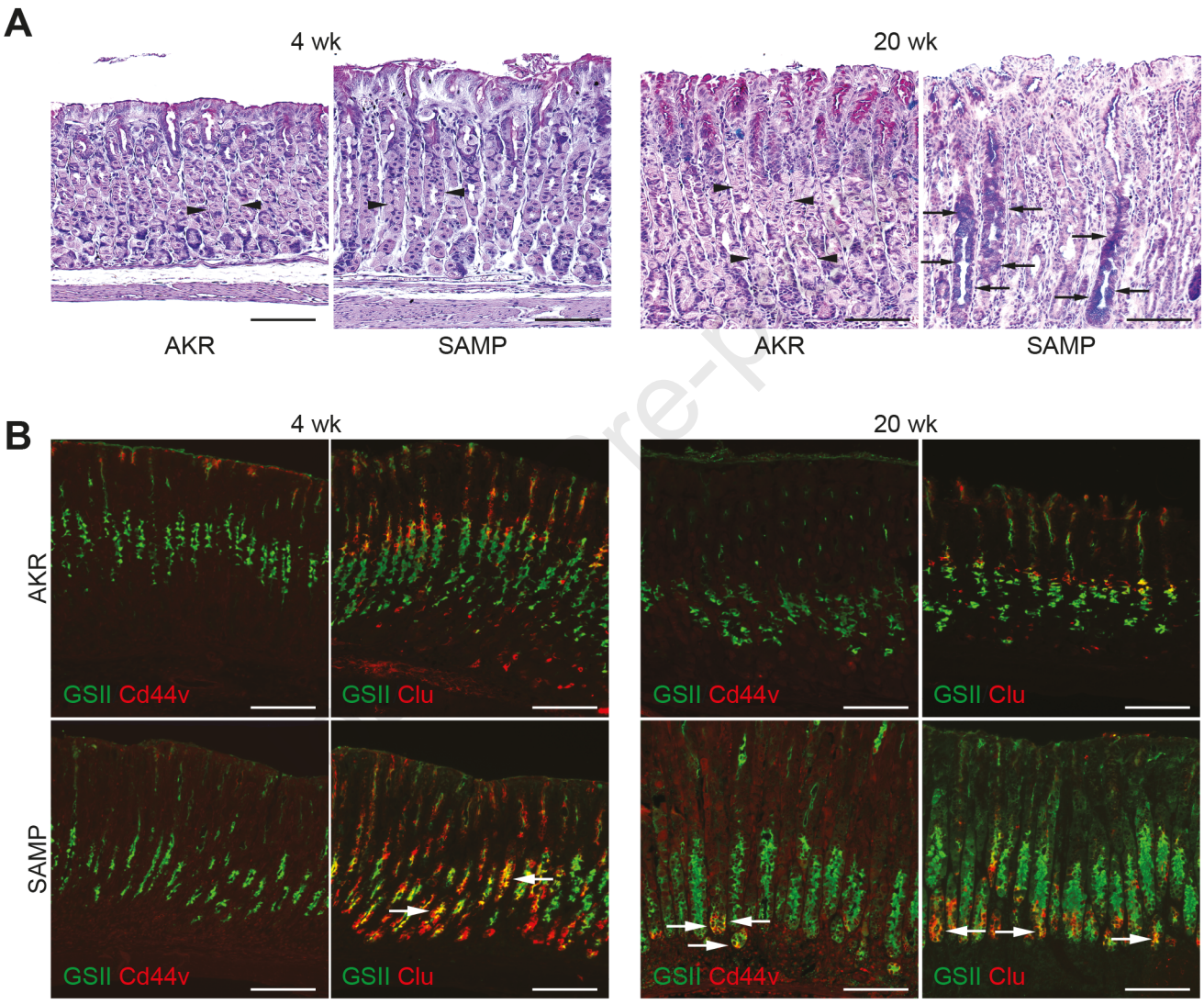

Supplemental Figure 1

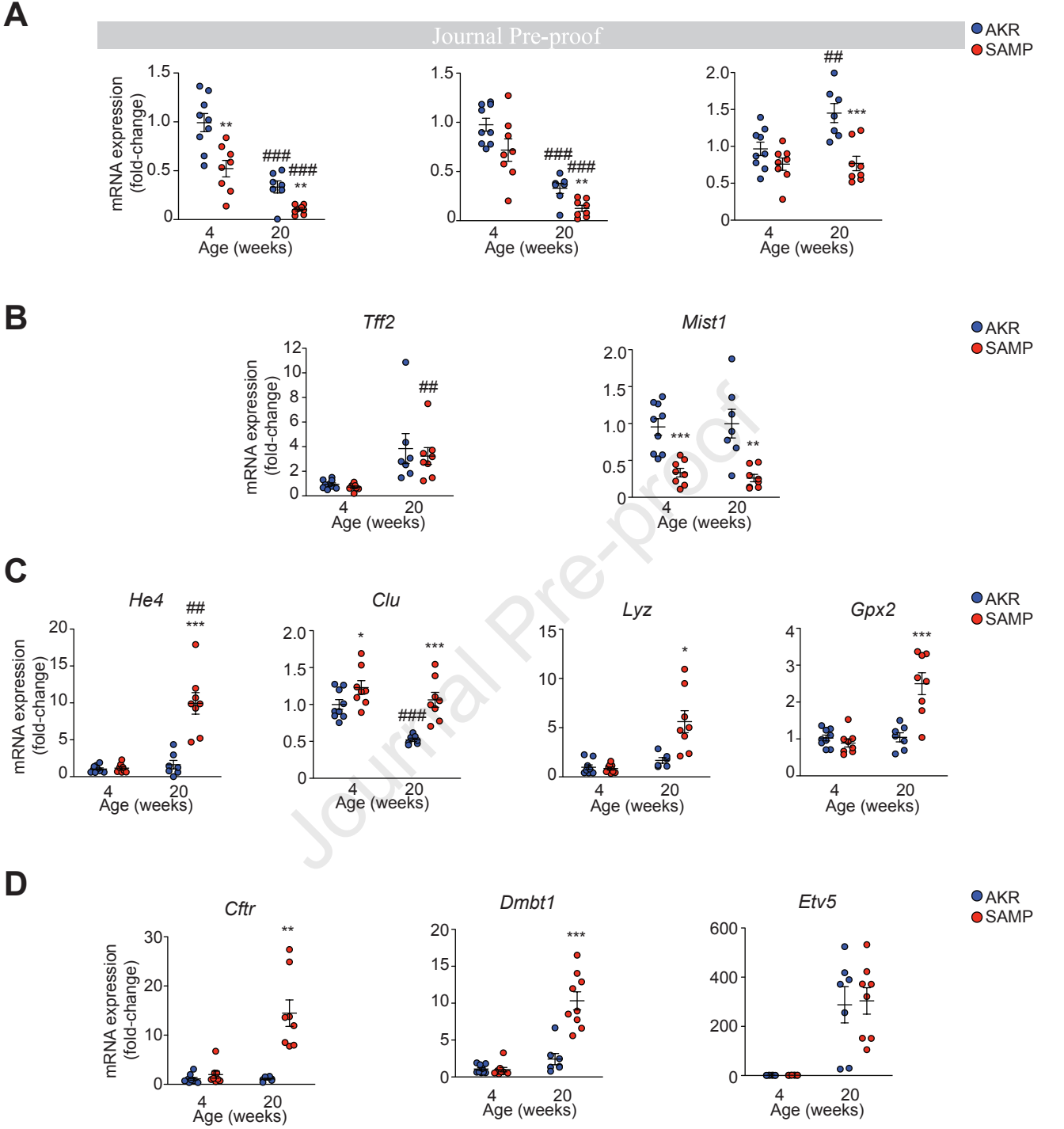

Supplemental Figure 2

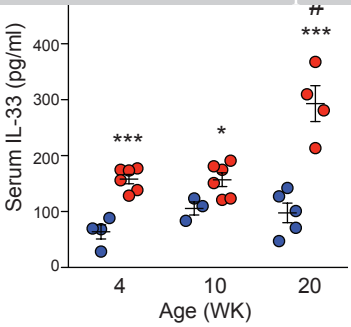

Supplemental Figure 3

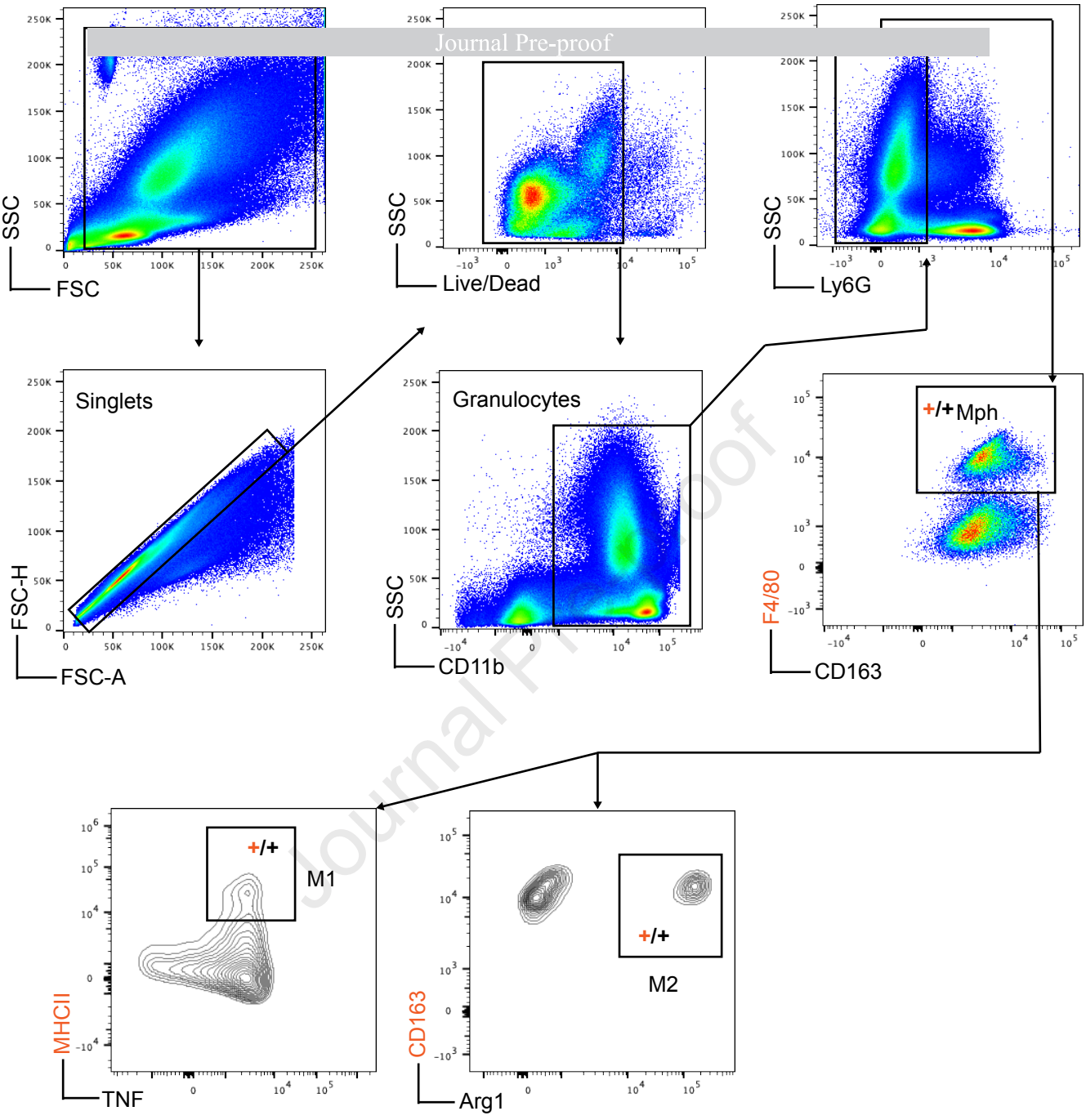

Supplemental Figure 4

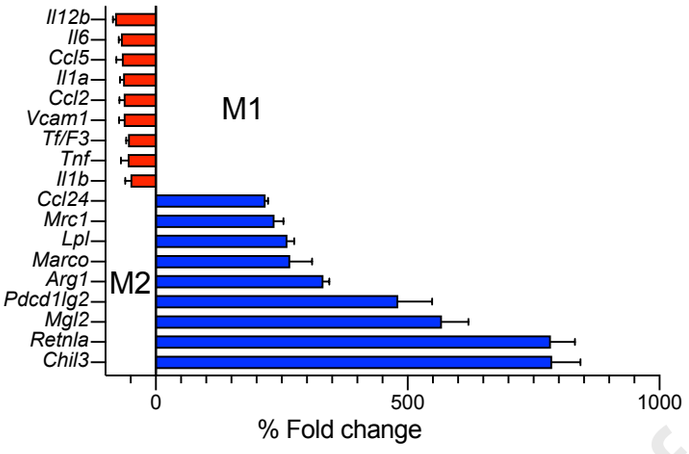

Supplemental Figure 5

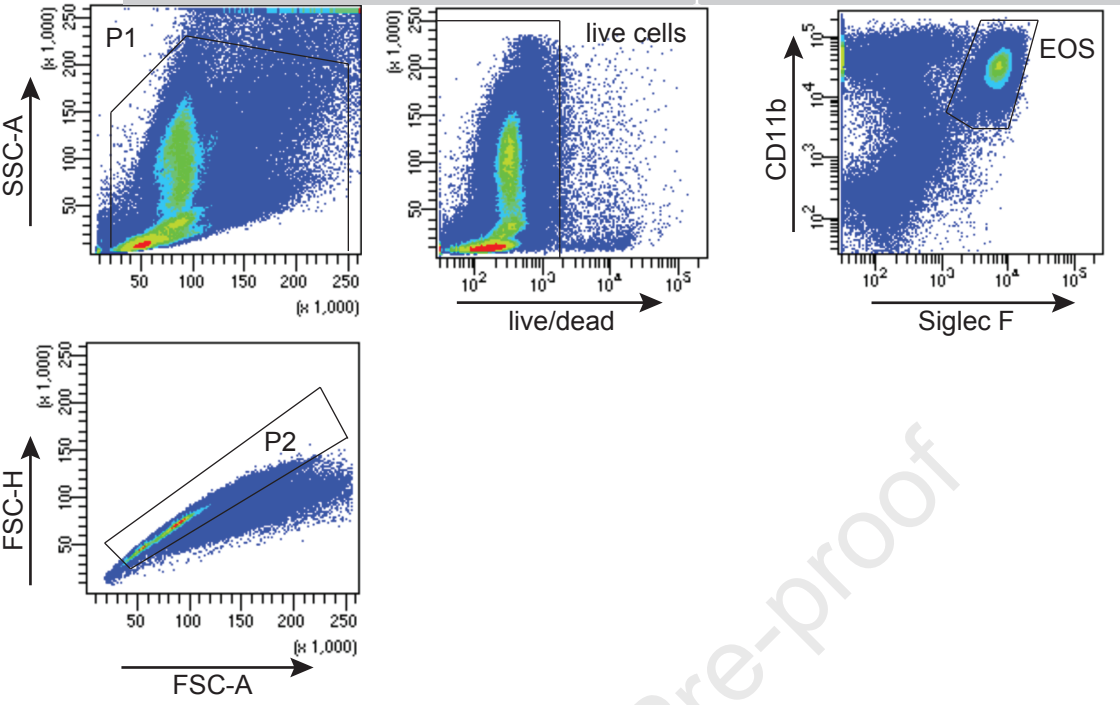

Supplemental Figure 6

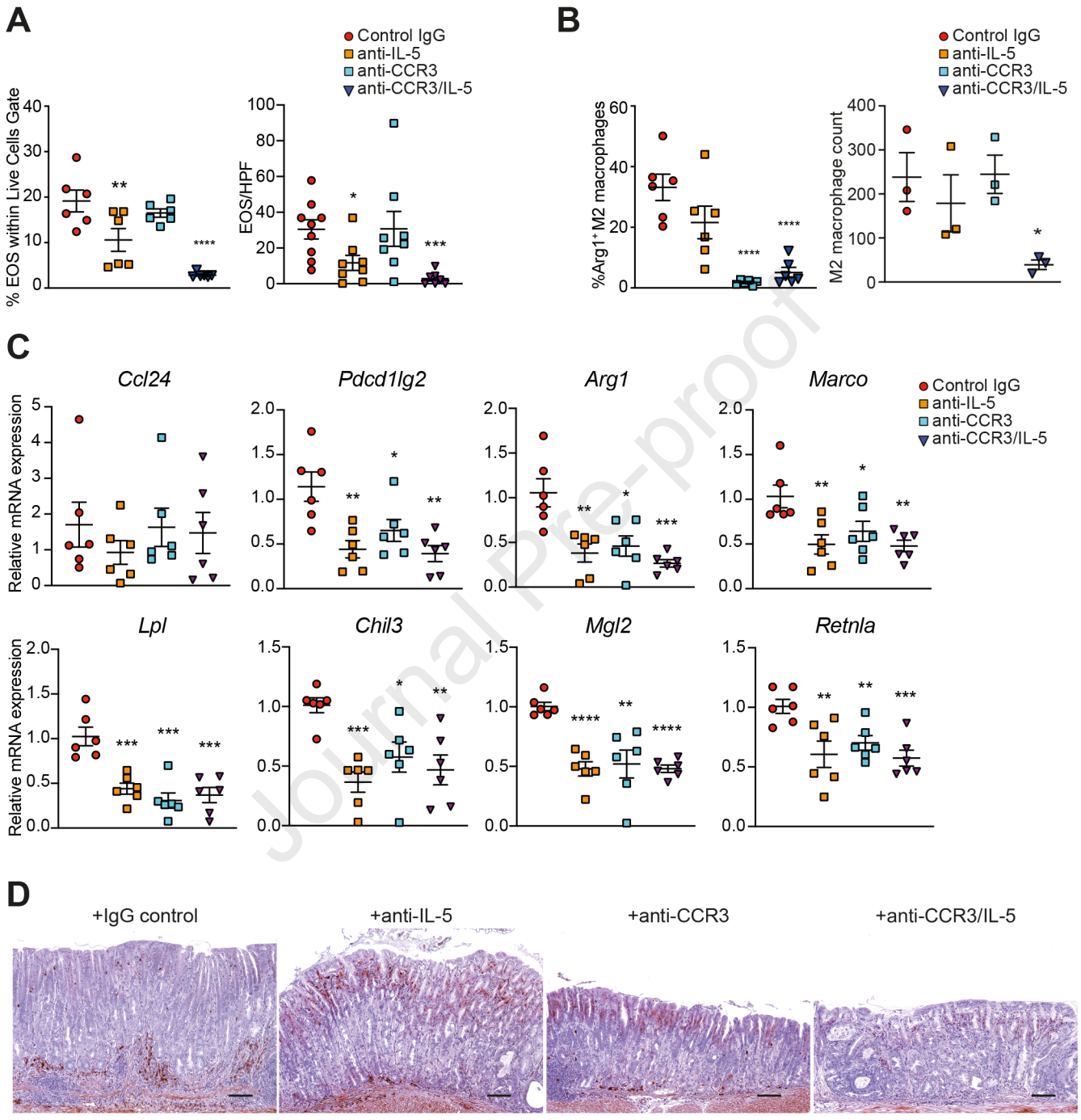

Supplemental Figure 7

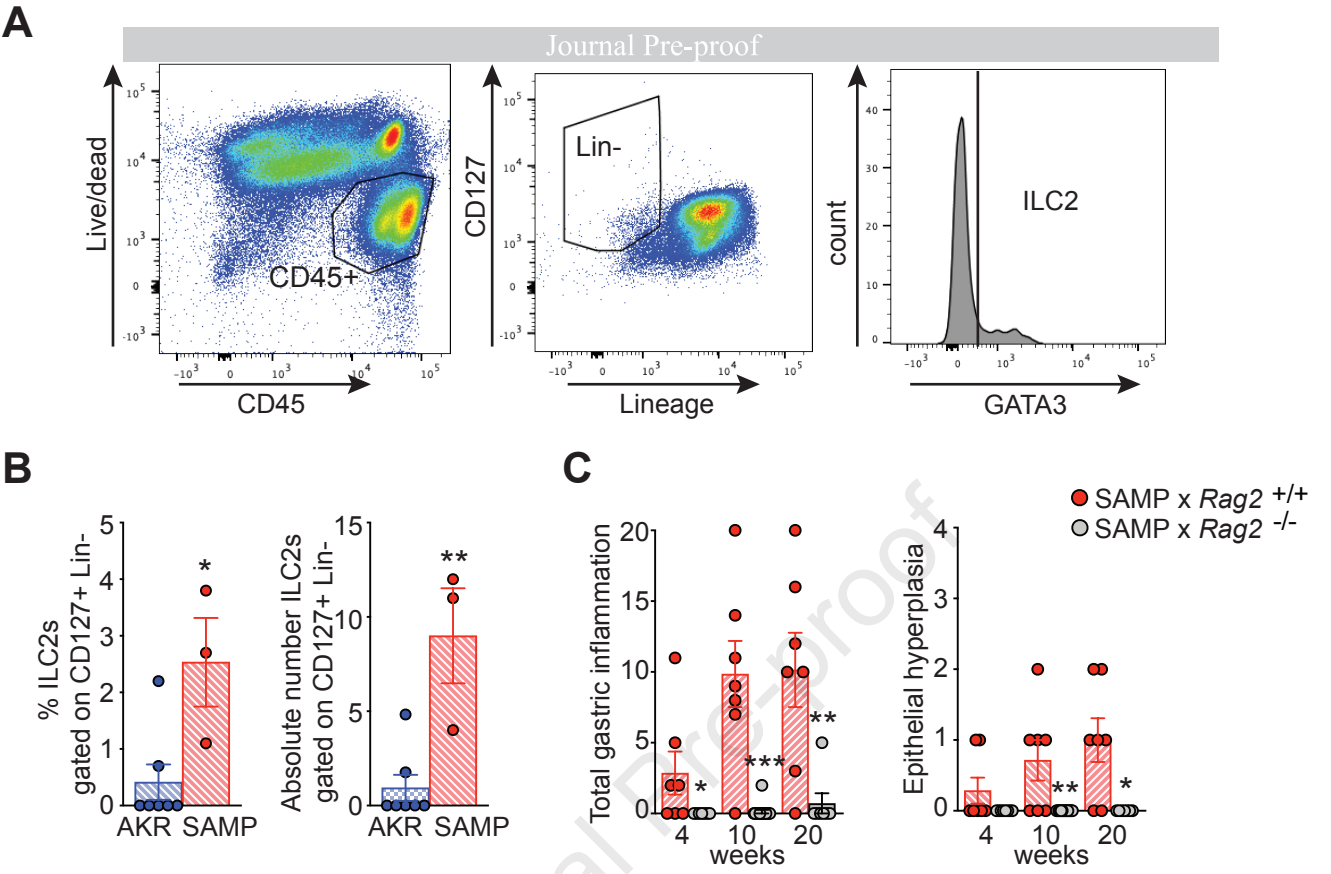

Supplemental Figure 8

Supplemental Table 1. *Primer sequences for qPCR analyses*

Target	Sequence fwd	Sequence rev
Actinb	5'-CAGGGTGTGATGGTGGGAATG-3'	5'-GTAGAAGGTGTGGTGCCAGATC-3'
Tff1	5'-AGCACAAGGTGATCTGTGTCC-3'	5'-GGAAGCCACAATTTATCCTCTCC-3'
Tff2	5'-TGCTCTGGTAGAGGGCGAG-3'	5'-CGACGCTAGAGTCAAAGCAG-3'
Mist1	5'-TGGTGGCTAAAGCTACGTGTC-3'	5'-GACTGGGGTCTGTCAGGTGT-3'
Atp4a	5'-TCTGCTTTGCGGGACTTGTA-3'	5'-CGGCATTTGAGCACAGCAT-3'
Lyz	5'-GAGACCGAAGCACCGACTATG-3'	5'-CGGTTTTGACATTGTGTTCGC-3'
Gif	5'-CCCTCTACCTCCTAAGTGTTCTC-3'	5'-CTGAGTCAGTCACCGAGTTCT-3'
He4	5'-AACCAATTACGGACTGTGTGTT-3'	5'-TCGCTCGGTCCATTAGGCT-3'
Dmbt1	5'-ACCTCCTCACGGTGCTACAG-3'	5'-GCTTCTTCACATCCTCCACTG-3'
Cftr	5'-CTGGACCACACCAATTTTGAGG-3'	5'-GCGTGGATAAGCTGGGGAT-3'
Gpx2	5'-CAGGGCTGTGCTGATTGAG-3'	5'-CGGACATACTTGAGGCTGTTC-3'
Clu	5'-CCAGCCTTTCTTTGAGATGA-3'	5'-CTCCTGGCACTTTTCACACT-3'
Etv5	5'-GCTCTTGGTGCTAAGTAGGA-3'	5'-TCTGATGGGTGGGTGACA-3'
Il33	5'-TCCTTGCTTGGCAGTATCCA-3'	5'-TGCTCAATGTGTCAACAGACG-3'
Il1rl1(ST2L)	5'-TGCGTACATCATTTACCCTCGGGTC-3'	5'-TCTTGTGCCACAAGAGTGAAGTAGG-3'
Il1rl1(sST2)	5'-ACGCTCGACTTATCCTGTGG-3'	5'-CAGGTCAATTGTTGGACACG-3'
Ccl24	5'-ATTCTGTGACCATCCCCTCAT-3'	5'-TGTATGTGCCTCTGAACCCAC-3'
Pdcd1lg2	5'-TGTGCTGCCTTTTCTGTGTC-3'	5'-GCAGCATGGTCTGTGTCAAT-3'
Arg1	5'-TTTTAGGGTTACGGCCGGTG-3'	5'-CCTCGAGGCTGTCCTTTTGA-3'
Marco	5'-GCACTGCTGCTGATTCAAGTTC-3'	5'-AGTTGCTCCTGGCTGGTATG-3'
Lpl	5'-GTGGCCGAGAGCGAGAAC-3'	5'-AAGAAGGAGTAGGTTTTATTTGTGGA-3'
Chil3	5'-CAGGTCTGGCAATTCTTCTGAA-3'	5'-GTCTTGCTCATGTGTGTAAGTGA-3'
Mgl2	5'-TTAGCCAATGTGCTTAGCTGG-3'	5'-GGCCTCCAATTCTTGAAACCT-3'
Retnla	5'-CCCTCCACTGTAACGAAGACTC-3'	5'-CACACCCAGTAGCAGTCATCC-3'
Mrc1	5'-GGACGAGCAGGTGCAGTT-3'	5'-CAACACATCCCGCCTTTC-3'
Il1a	5'-GCACCTTACACCTACCAGAGT-3'	5'-AAACTTCTGCCTGACGAGCTT-3'
Il1b	5'-GCAACTGTTCCTGAACTCAACT-3'	5'-ATCTTTTGGGGTCCGTCAACT-3'
Tnf	5'-CCCTCACACTCAGATCATCTTCT-3'	5'-GCTACGACGTGGGCTACAG-3'
Vcam1	5'-ACGTCAGAACAACCGAATCC-3'	5'-GTGGTGCTGTGACAATGACC-3'
Il12b	5'-TGGTTTGCCATCGTTTTGCTG-3'	5'-ACAGGTGAGGTTCACTGTTTCT-3'
Il6	5'-TAGTCCTTCCTACCCCAATTTCC-3'	5'-TTGGTCCTTAGCCACTCCTTC-3'
Ccl5	5'-GCTGCTTTGCCTACCTCTCC-3'	5'-TCGAGTGACAAACACGACTGC-3'
Ccl2	5'-TTAAAAACCTGGATCGGAACCAA-3'	5'-GCATTAGCTTCAGATTTACGGGT-3'
Tf/F3	5'-CCGAGCAATGGAAGAGTTTC-3'	5'-CGCTTGCACAGAGATATGGA-3'
36B4	5'-GCTCCAAGCAGATGCAGCA-3'	5'-CCGGATGTGAGGCAGCAG-3'

Supplemental Table 2. *Antibodies utilized for flow cytometry*

Antigen	Label	Catalog #	Source
CD11c	PECy7	561241	BD Biosciences, San Jose, CA
CD11b	PE-CF594	562287	BD Biosciences
F4/80	Alexa-488	564227	BD Biosciences
Ly6G	BUV396	563978	BD Biosciences
Siglec F	BV610	740280	BD Biosciences
MHCII	BV711	563414	BD Biosciences
Arginase 1	APC	17-3697-82	ThermoFisher, Waltham, MA
TNF	BV650	563943	BD Biosciences
CD163	BV421	155309	Biolegend, San Diego, CA
IL33	PE	MA5-23640	ThermoFisher

“What you Need to Know”

Background and Context: The link between chronic, non-resolving inflammation and cancer is well established, with inflammation-associated cancers among the most highly represented and frequently-occurring neoplasias worldwide. Investigation over the last several years has focused on determining critical pathways involved in this process, with a number of candidate molecules identified, including members of the interleukin-1 (IL-1) family that are particularly important in cancers of the GI tract.

New Findings: IL-33 (or IL-1F11), a member of the IL-1 family of cytokines, serves as an important mediator linking chronic inflammation and metaplasia by inducing the expansion and recruitment of activated eosinophils leading to advanced, intestinalized SPEM in gastritis-prone SAMP1/YitFc (SAMP) mice.

Limitations: Further studies are warranted to determine the precise inciting factors of increased IL-33 leading to intestinalized SPEM in SAMP mice, as well as in patients with gastric cancer.

Impact: The present manuscript contributes to a better understanding of potential mechanism(s) that promote the inflammation-metaplasia-dysplasia-carcinoma sequelae that can apply to several GI-related cancers.

Lay Summary

IL-33-activated eosinophils are important in the early cascade of events leading to intestinalized metaplasia in gastritis-prone mice, and represents a potential mechanism that promotes the inflammation-metaplasia-dysplasia-carcinoma sequelae.